BRNO UNIVERSITY OF TECHNOLOGY
VYSOKÉ UČENÍ TECHNICKÉ V BRNĚ

FACULTY OF MECHANICAL ENGINEERING
FAKULTA STROJNÍHO INŽENÝRSTVÍ

INSTITUTE OF AEROSPACE ENGINEERING
LETECKÝ ÚSTAV

OPTIMAL MODELLING OF RIVET JOINTS USING FINITE ELEMENT METHOD
OPTIMÁLNÍ MODELOVÁNÍ NÝTOVÉHO SPOJE POMOCÍ METODY KONEČNÝCH PRVKŮ

MASTER'S THESIS
DIPLOMOVÁ PRÁCE

AUTHOR — **BEng. Ioseb Giorgobiani**
AUTOR PRÁCE

SUPERVISOR — **Ing. Jaroslav Bartoněk**
VEDOUCÍ PRÁCE

BRNO 2020

BRNO UNIVERSITY OF TECHNOLOGY
FACULTY OF MECHANICAL ENGINEERING

Specification Master's Thesis

Department:	Institute of Aerospace Engineering
Student:	**BEng. Ioseb Giorgobiani**
Study programme:	Mechanical Engineering
Study branch:	Aircraft Design
Supervisor:	**Ing. Jaroslav Bartoněk**
Academic year:	2019/20

Pursuant to Act no. 111/1998 concerning universities and the BUT study and examination rules, you have been assigned the following topic by the institute director Master's Thesis:

Optimal modelling of rivet joints using finite element method

Concise characteristic of the task:

Research of methods of rivet joint modelling with using the PATRAN/NASTRAN software. Evaluation according to selected criteria. Experimental validation of results.

Goals Master's Thesis:

1. Create a list and detailed description of several forms of representation of rivet joints on aerospace structures using PATRAN/NASTRAN software.

2. List strong and weak points of each form. Define the situations these forms are optimal for and provide the criteria for their evaluation. Do not forget their limits.

3. Select at least one typical rivet joint. Perform the static check using the selected methods of finite element modelling. Then perform a static test of this joint with real specimen. Compare and evaluate the results.

Recommended bibliography:

NIU, Michael Chun-Yung. Airframe structural design. 2nd ed. Hong Kong: Hong Kong Conmilit Press, 2004, 612 s. ISBN 962-7128-09-0.

BRUHN, Elmer Franklin. Analysis and design of flight vehicle structures. Cincinnati: Tri-State Offset Co, [1965].

Deadline for submission Master's Thesis is given by the Schedule of the Academic year 2019/20

In Brno,

L. S.

doc. Ing. Jaroslav Juračka, Ph.D. Director of the Institute	doc. Ing. Jaroslav Katolický, Ph.D. FME dean

Abstract

The thesis in focused on finding optimal model for three different configuration rivets in MSC Nastran/Patran software. With the outcome of this findings it will be possible to virtually check engineers understanding of rivet joints behavior under some load, in order to take another step which is the case of real static tests. By inserting Finite Element Analysis step in products certification protocol, time and budget consuming static test can be reduced to the minimum. If an engineer could better understand structure's behavior, there would be much less chance of it to collapse earlier than expected load.

Key words

FEM, Rivet joint, MSC Nastra/Patran, CBUSH element, CBEAM element, RBE elements,

GIORGOBIANI, Ioseb. Optimal modelling of rivet joints using finite element method. Brno, 2020. Dostupné také z: https://www.vutbr.cz/studenti/zav-prace/detail/125203. Master's Thesis. Vysoké učení technické v Brně, Fakulta strojního inženýrství, Institute of Aerospace Engineering. Supervisor Jaroslav Bartoněk.

I hereby declare that I am the sole author of this master's thesis and that I have not used any sources other than those listed in the bibliography and identified as references. I further declare that I have not submitted this thesis at any other institution in order to obtain a degree.

BEng. Ioseb Giorgobiani

Acknowledgement

I would like to thank to PhD. Teimuraz Lomtadze from Technology Institute of Georgia, for funding my whole master's study therefore giving me valuable lifetime experience, also to my supervisor Ing. Jaroslav Bartoněk for his professional guidance and support (especially during pandemic). Also want to thank to all the employees of Brno university of Technology, who were involved in my studies. Last, but definitely not least, I thank to my family for the encouragement through my studies. Well, and to me for always having faith in me.

BEng. Ioseb Giorgobiani

Content

1. Introduction

The testing of the structures is one of the most expensive and time-consuming step of the manufacturing and the reason for that is certification of those structures, which consists, making number of prototypes and testing them under needed environments and conditions (The Problem). Apart from checking quality of raw material or the work done, engineers analisys are also checked and in particular how would they understand the behavior of the structure under known stresses, had they predicted all the crucial sections of the product and most importantly, how efficiently was the structure designed.

Over time to time engineers from various fields and mathematicians made or improved couple of tools or methods to reduce mentioned disadvantages, for example by choosing the better or by modifying the existing technology, which reduced time and cost of the product. Another approach is using numerical method and specifically Finite Element Analysis (FEA), which gives opportunity to engineers to virtually test mentioned structure under the different environment or the different load. This would give a chance to the engineers to see how the structure would deform under the different loadings.

FEA uses a complex system of points (nodes), making up a grid called a mesh. The mesh is programmed to contain all the material properties, and other factors that constitute the structure and determine how it would react to the certain load conditions, such as thermal, gravitational, pressure, or point loads. The elements are then assigned a density throughout the material, all depending on the stress levels anticipated in a certain area. In general, points with more stress (such as corners of a building or contact points on a car frame) will usually have a higher node density than those with little or no stress. As researchers examine the results of the FEA, they learn how the structure responds to the various loads, which gives an opportunity to the engineers to see which part of the structure must be modified in order to achieve the best result in creating the final product.

The purpose of this paper is to find optimal modeling ways for rivet joints in MSC, Nastran/Patran software, which can reduce the traditional time-consuming procedures in real production to the minimum. In a classic scenario, the ordinary rivet joint assemblies require several static, dynamics or fatigue tests. This paper will try to discuss specific rivet joint that is calculated with the analytical way. Simultaneously, the latter will be made model for that joint in the software and finally, the structures will also be tested. All the final results will be compared to each other to find how accurate Finite Element (FE) model is made.

The first part of the thesis presents the review of standardization of metal fastener joint, moreover, what recommendations must be taken into account, also the descriptions of a rivet and what approaches must be done for the traditional calculations.

The thesis later continues with detailed descriptions of each rivet joint traditional analysis and their FE models.

In the final - third part of the paper the results from the static tests of the mentioned joint shall be discussed.

2. Limitations

The Mentioned Problem in the introduction consists of the modelling and testing of the different types of joints failure, which leads quite a complex data that requires number of different testing. Due to the fact that we are limited in terms of the time and the devices and the considering the fact that there are several types of failures of the rivet joint, in this paper, I shall discuss only the rivet static shearing failure of the single lap joint with the different configurations. Furthermore, applying FE analysis is yet new tool for the engineers. Moreover, it should be outlined that the latter concept is still being modified/upgraded, therefore there is not much information/articles, sources or findings about its features and characteristics.

3. Standardization of the metal fastener

3.1. Metal fastener Joint

A complete airplane structure is manufactured from many parts. These parts are made from different type of raw material like: sheets, extruded sections, forgings, castings, tubes or machined shapes which must be joined together to form subassemblies. The subassemblies must then be joined together to form larger assemblies and then finally assembled into a completed airplane. Example is shown in Figure 1.

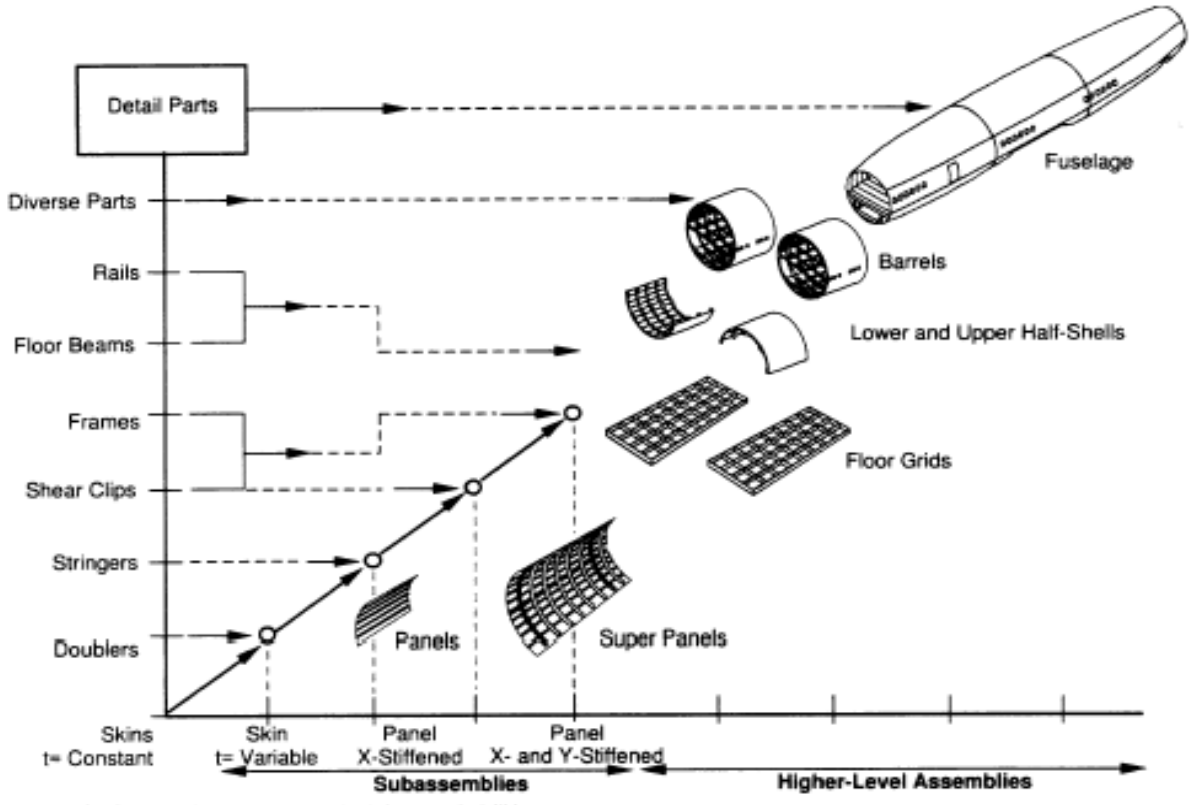

Figure 1. Assembly of a fuselage

Many parts of the completed airplane must be arranged so that they can be disassembled for shipping, inspection, repair or replacement and are usually joined by bolts or rivets. In order to facilitate the assembly and disassembly of the airplane, it is desirable for such bolted or riveted

connections to contain as few fasteners as possible for example, a semi monocoque metal wing usually resists bending stresses in numerous stringers and sheet elements distributed around the periphery of the wing cross section. The wing usually is not made as one continuous riveted assembly from tip to tip, but must usually be spliced at two or more cross sections in Figure 2.

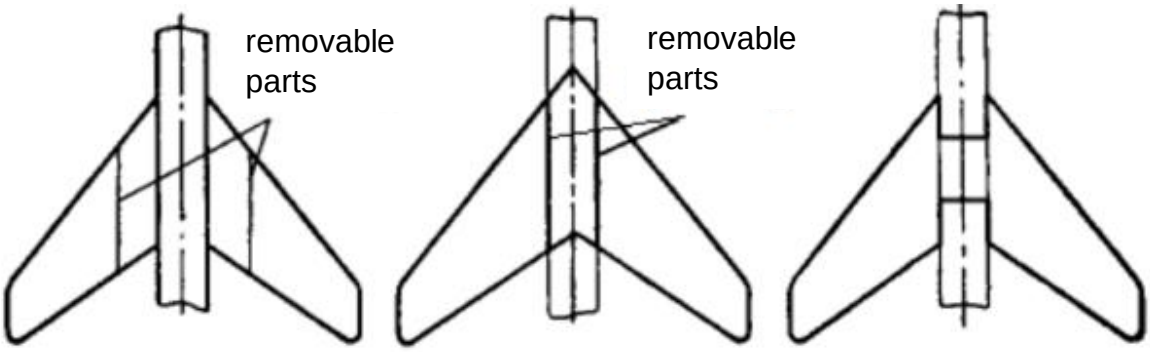

Figure 2 Cross sections

These splices are often designed so that four bolts, for example, transfer all the loads across splice. These bolts connect members called fittings, which are designed to resist the high concentrated loads and to transfer them to the spars, from which the loads are distributed to the sheet and stringers. The entire structure for transferring the distributed loads from the sheet and stringers outboard of the splice into a concentrated load at the fitting and then splice into a concentrated load at the fitting and then distribute this load to the sheet and stringers inboard of the splice is considerably heavier than the continuous structure which would be required if there were no splice. Many uncertainties exist concerning the stress distribution in fittings. According [5] (Agency, 2012, p. 57), The fitting factor (15%) must be used in the designing the entire fitting, including bolted riveted or welded joint attaching the fitting to the structural members. The fitting factor need not to be used in designing a continuous riveted joint.

The ideal aircraft structure would be a single complete unit of the same material involving one manufacturing operation. Unfortunately, the present-day types of materials and their method of working dictates a composite structure. Furthermore, general requirements of repair, maintenance and stowage dictate a structure of several main units help to other units by main primary fittings or connections, with each unit incorporating many primary and secondary connections involving fittings, bolts, rivets, welding, etc. No doubt main or primary fittings involve more weight and cost per unit volume than any other part of the aircraft structure, and therefore, fitting and joint design plays an important part in aircraft structural design (Niu, 1988, p. 207).

3.2. General design considerations

According [1] (Niu, 1999, pp. 273-278) Joints are perhaps the one of the most common failure in aircraft structure and therefore it is the most important that all aspects of the design are given consideration when making the structural analysis. Failures may occur for various reasons but generally because of some factor, such as secondary stresses due to eccentricities, stress concentrations, slippage of connectors, excessive deflections, etc. or some combination of conditions, all of which are difficult to evaluate to an exact degree. These factors not only affect

the static strength but have a great influence on the fatigue life of the joint and the adjacent structure.

1. Fitting factor:
   An Ultimate fitting factor of 1.15 shall be used in the joint analysis:
   a) This factor of 1.15 shall apply to all portions of the fitting including the fastening and bearing on the joined member.
   b) For each integral fitting, the part must be treated as a fitting up to the point at which the section properties become typical of the member.
   No fitting factor need be used:
   a) For joints made under approved practice and based on comprehensive test data
   b) with respect to any other design factors for which a larger special factor is used.

2. Overall joint efficiency:
   It is a primary consideration that the strength of the joint will be equal to or greater than that of the parent structure. One side of the joint should not be designed for maximum efficiency at the expenses of a weight and fabrication cost penalty one the other. The joint should be located at support structures such as stringers, stiffeners, bulkheads, etc. to improve joint efficiency as shown in Figure 3.

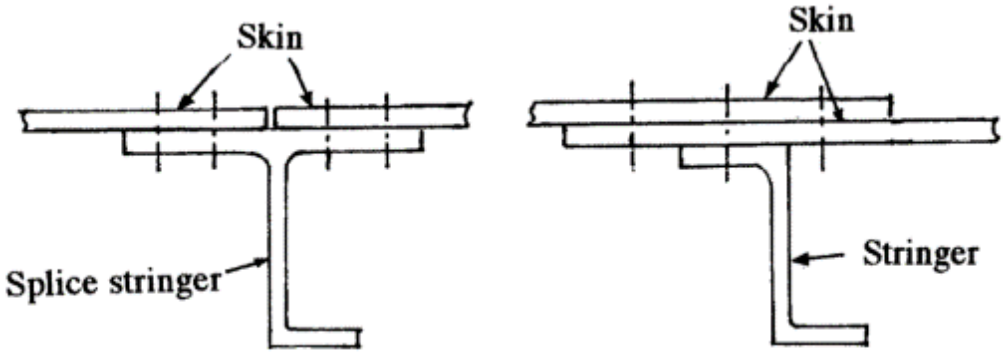

Figure 3. Supported joints

3. Eccentricities and their effect on the part of the joint and the surrounding structure. If eccentricities exist in a joint the moment they produce must be resisted by the adjacent structure. When a joint contains a dihedral angle (such as wing structure), a rib should be provided at the vertex of the angle to eliminate the eccentricity that would exist. A joint of a truss structure containing an eccentricity produces secondary stresses which would be accounted for. Eccentricity loaded bolt and rivet patterns may produce excessively loaded connectors if eccentricity is not considered.
4. Fatigue considerations.
5. Mixed fasteners:
   It is not good practice to employ both rivets and bolts in combination in a joint. Due to a better fit for the rivets, the bolts will pick up their proportionate share of the load until the rivets have deflected enough to take up the clearance of the bolts in their bolt holes. this

tends to overload the rivets and may induce premature failure. If such a combination is absolutely necessary, it is advisable to use close tolerance bolts in reamed holes.

6. Splices in discontinuous members, which act in conjunction with a part or parts which are continuous past the splice, should be made as rigid as possible using generous splice members and close-fitting attachments, thereby minimizing slippage which might overload the continuous material and cause premature failure.
7. insufficient rigidity of surrounding structure may cause excessive deflections and consequent changes in direction and magnitude of load on certain joints, such as those in a landing gear installation.
8. Do not use spot welds on either side at the joggled area of joggled member, use rivets at the joggle.
9. Do not use a long string of fasteners in a splice. In such cases, the end fasteners will load up first and yield early. Three, or at most four fasteners per side is upper limit unless a carefully tapered, thoroughly analyzed splice is used.
10. Carefully insure against feather edges in all joint designs the thickness of countersunk sheet shall be equal to or greater than 1.5 times the depth of the countersunk head of the fastener at the fatigue critical areas. For other applications t≥ h+0.02 inch shall be considered (Figure 4).

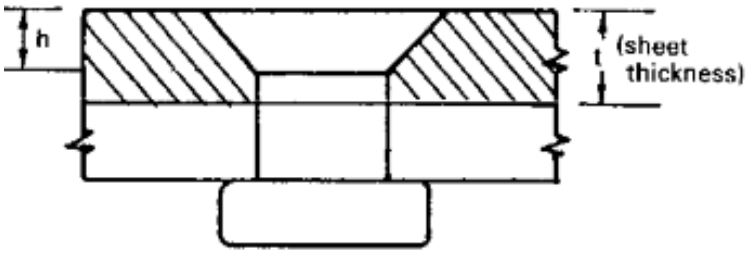

Figure 4. Feather-edge in countersunk sheet

11. When possible use a double shear splice.
12. Probably the most single important item regarding detail structural design is the matter of equilibrium. If the engineer will show the load in equilibrium for every part of the assembly, most errors will be prevented.
13. Carefully selected interference-fit fasteners which produce sustained tensile stress (stress corrosion crack in fastened material).
14. Fastener spacing and edge distance $\left(\frac{e}{D}\right)$:

In normal metallic sizing, the minimum fastener spacing (pitch) is 4D and edge distance in the direction of load is $\frac{e}{D} = 2.0$ (D is diameter of the fastener and e is the distance from the center of the fastener to edge of the part plus an additional margin of 0.03inch for tolerance and misdrill) as shown in Figure 5. Minimum edge distance $\frac{e}{D} = 1.5$, may be used, provided the following criteria are met:

a) Low load transfer such as spar or rib vertical stiffener attached to web

b) Assume non-buckled skin.

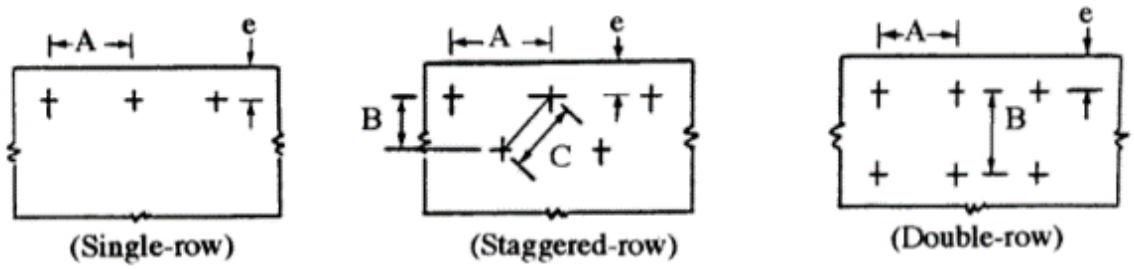

Figure 5. Fastener spacing

15. The use of rivets involving tension only is poor engineering practice and should be held to a minimum. (Niu, 1999, pp. 274-277)

When secondary tension loads are improved on a standard aluminum rivet (such as the attachment of a diagonal tension web to a stiffener), use the tension allowable of rivet and sheet combination test allowable data.

3.3. Rivets (permanent fasteners)

Rivets are low cost, permanent fasteners well suited to automatic assembly operations. The primary reason for riveting is low in-place cost, the sum of initial rivet cost and costs of labor and machine time to set the rivets in the parts. Initial cost of rivets is substantially lower than that of threaded fasteners because rivets are made large volumes on high-speed heading machines, with little scrap loss. Assembly costs are low. Rivets can be clinched in place by high-speed automatic machinery.

Advantages:

- High reliability, because of longtime experience.
- Dissimilar materials, metallic or nonmetallic, in various thickness can be joined any material that can be cold worked makes a suitable rivet.
- Rivets may have a variety of finishes such as plating, Parkerizing or paint.
- Parts can be fastened by rivet, if parallel surfaces exist for both the rivet driver during clinching.
- Rivets can serve as fasteners, pivot shafts, spacers, electric contacts, stops or inserts.
- Parts that are painted or have received other finishes can be fastened by rivets.

Disadvantages:

- Rivet holes decrease strength of the sheet, plus apart from adhesive joint load distribution on rivet joint is not uniform Figure 6.
- Tensile and fatigue strength of rivets are lower than comparable bolts or screws. High tensile loads may pull out the clinch or severe vibrations may loosen the fastening. Riveted joints are normally neither watertight nor airtight; however, such joints may be attained, at added cost, by using a sealing compound.
- Riveted parts cannot be disassembled for maintenance or replacement without destroying the rivet.
- Rivets produced in volume are not normally made with the same precision as screw-machine parts.
- A weight penalty. (Niu, 1988, p. 210)

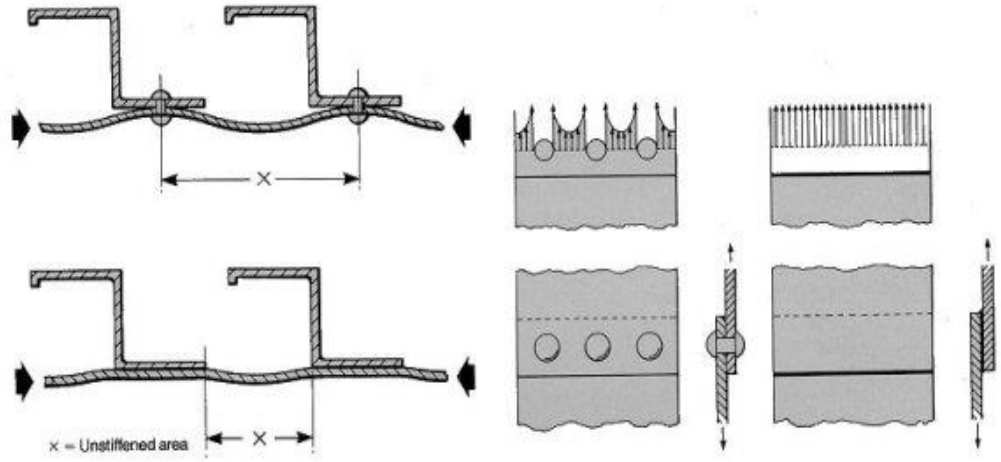

Figure 6. Comparison of riveted and adhesive bonded joint

3.4. Types of Failure

A riveted join may fail in several ways but the failure occurs as soon as failure takes place in any one mode. Following is the description of modes of failures of a riveted joint. These modes are described with the help of a single riveted lap joint, which is subjected to tensile load P, in general the description will be applicable to any other type of joint.

a) Tearing of plate at the section weakened by holes (Figure 7).
The plate at any other section is obviously stronger and hence does not fail. If tensile force P is to cause tearing, it will occur along weakest section, which carries the row of rivets. If only one pitch length p is considered; it is weakened by one-hole diameter d. The area that resists the tensile force is: $A_t = (p - d)t$, where t is thickness if the plate. If the permissible stress for plate in tension is σ_t, then tensile strength of the joint or tensile load carrying capacity of the joint: $P_t = \sigma_t(p - d)t$. If P is the applied tensile force per pitch length then the joint will not fail if $P_t \geq P$.

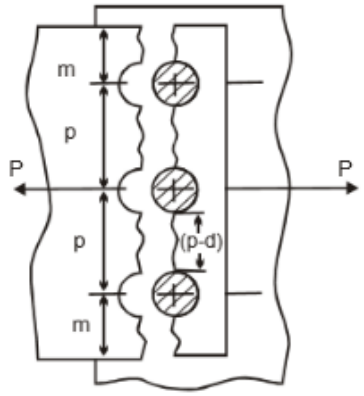

Figure 7. Tension failure

b) Shearing of rivet (Figure 8).
According [3] (Dimarogonas, 2001, pp. 512-513), When a transverse Force F is acting on cross-sections of a bar and the other internal forces are equal to zero, this type of loading is called shear, in this case only shearing stresses arise at the section. In most practical problems, a transverse force acts simultaneously with a bending moment and a longitudinal force so that normal stresses as well as shearing stresses usually act over the cross-sections. However, in cases where shearing strength analysis needs to be considered in the design. A typical example of such a simplified but, as experience shows, quite reliable analysis is the calculation of the shear strength of riveted, bolted and welded joints.
The failure will occur when all the rivets in a row shear off simultaneously. Considers the strength provided by the rivet against this mode of failure. In a lap joint failure due to shear may occur only along one section of rivet as shown in Figure 8(a). However, in case of double cover butt joint failure may take place along two sections in the manner shown in Figure 8(b). So, in case of single shear the area resisting shearing of a rivet: $A_s = \frac{\pi}{4} d^2$ If permissible shearing stress in single shear of rivet is τ_s, then the shearing strength or shearing load carrying capacity of the joint: $P_s = \tau_s \frac{\pi}{4} d^2$. The failure will not occur if: $P_s \geq P$.
We may also write if n is the number of rivets per pitch length: $P_s = n \text{ x } \tau_s \frac{\pi}{4} d^2$
If the rivet is in double shear as in Figure 8(b) for preliminary analysis the effective area over which failure occurs in 2 As. Formula will be: $P_s = n \text{ x } \tau_s \frac{\pi}{2} d^2$

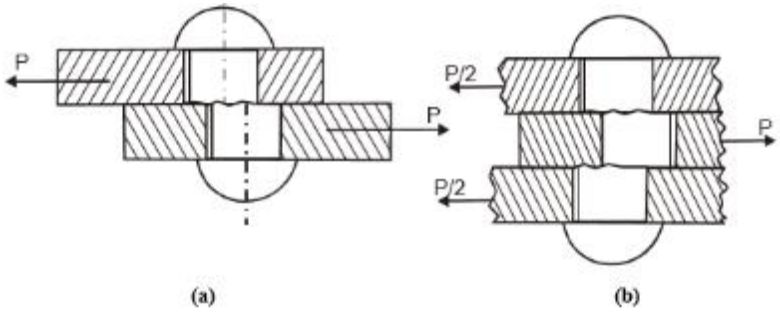

Figure 8. Shearing of rivet, a) single shear b) double shear.

There is one special case, when tension force is nominal direction to several rivet in single row. In this case, load distribution on rivets is depend on rivets relative stiffness, if rivets are extremely rigid, theoretically is considered that edge rivets would take maximum loads and middle ones will take 0, as flexibility of rivet increases shear load taken by middle rivets will increase (Figure 9), load distribution is also dependent on number of rivets (Figure 10), increased number of appropriate stiff rivets decreases load taken by edge rivets.

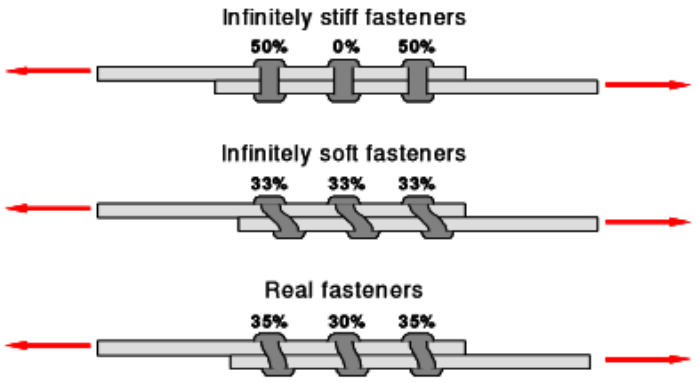

Figure 9. Load distribution on 3 rivets in series with different stiffnesses.

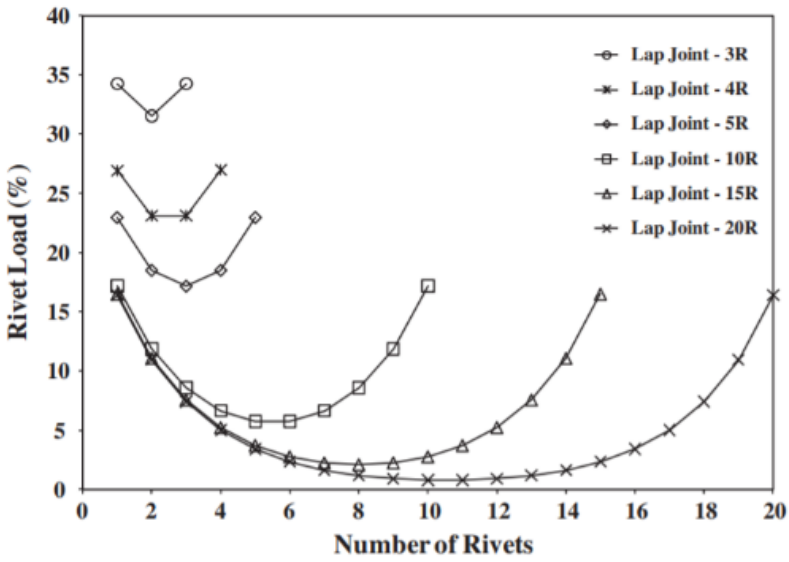

Figure 10. Load distribution on different number of rivets in series.

c) Crushing of plate and rivet (Figure 11)

Due to rivet being compressed against the inner surface of the hole, there is a possibility that either the rivet or mostly the hole surface may be crushed. The area, which resists this action, is the projected area of hole or rivet on diametral plane. The area per rivet is: $A_c = dt$. If permissible crushing or bearing stress of rivet or plate is σ_c the crushing strength of the joint or load carrying capacity of the joint against crushing is: $P_c = dt\sigma_c$. The failure will not occur if: $P_c \geq P$.

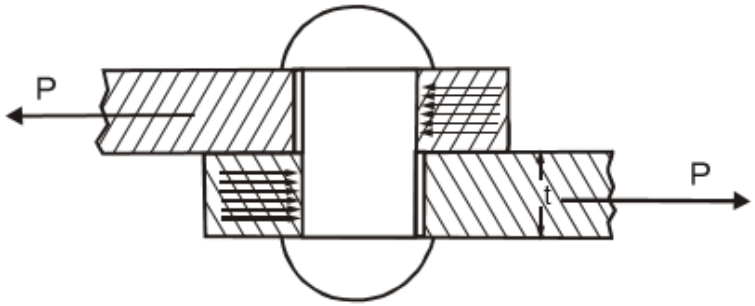

Figure 11. Crushing failure.

d) Shearing of plate margin near the rivet hole.
Figure 12 shows this mode of failure in which margin can shear along planes ab and cd, if the length of margin is m, the area resisting this failure is: $A_{ms} = 2mt$. If permissible shearing stress of plate is τ_s then load carrying capacity of the joint against shearing of the margin is: $P_{ms} = 2mt\tau_s$. The failure in this case will not occur if: $P_{ms} \geq P$, where P is the applied load per pitch length.

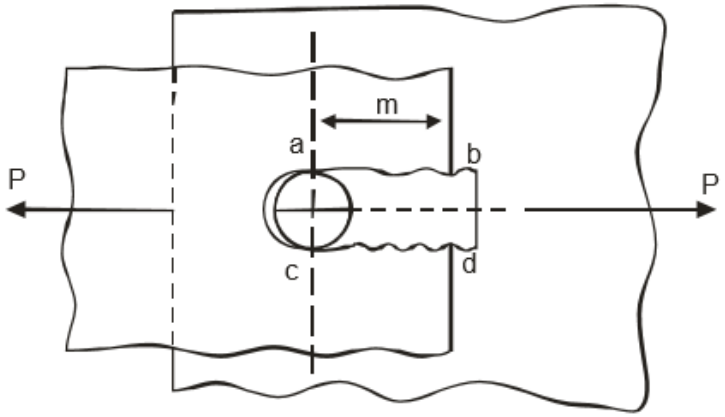

Figure 12. Shearing margin.

In writing down the above equations for strength of the joint certain assumptions have been made. It is worthwhile to remember them. Most importantly it should be remembered that most direct stresses have been assumed to be induced in rivet and plate which may not be the case. However, ignorance of actual state of stress and its replacement by most direct stress is compensated by lowering the permissible values of stresses σ_t, τ_s and σ_c, i.e. by increasing factor of safety.

4. Finite Element Method (FEM) element descriptions

4.1. Scalar elements

According [7] (Nastran, 2019, pp. 79-90), Scalar elements, also referred to as zero-dimensional elements, consists of the springs, masses, and viscous dampers. For static analysis the scalar spring is the most commonly used scalar element. The scalar elements used in static analysis consists of the following: CELASi, CBUSH, both as scalar spring element and CMASSi as scalar mass element, for this paper spring element is used, as spring elements defines structures' stiffness. Scalar elements do not require geometric and material inputs to calculate stiffness like 1,2 or 3-D elements do, instead of that, user him/herself inputs, in this case, spring constants, which are not dependent element length. CBUSH is updated version of CELASi, it gives opportunity to enter separate stiffnesses for all degree of freedom (3 translational and 3 rotational), while CELASi only defines stiffness in 1 degree of freedom.

Because CBUSH can define elements stiffness in all direction, in the models, which are mentioned in these papers, will be used CBUSH elements to represent rivets.

4.2. One-dimensional elements

According [7] (Nastran, 2019, pp. 90-134), The one-dimensional elements are used to represent structural members that have stiffness along a line or curve between two grid points. Typical applications include beam type structures, stiffeners, tie-down members, supports, mesh transitions and many others. The one-dimensional elements are: CROD, CBAR, CBEAM and CTUBE, etc.

The CROD elements is useless under shear load as, it only works under axial forces and doesn't have shear stiffness, this element is good to represent truss element structure, where structure parts are only under either tension or compression.

The CBAR element is a straight one-dimensional element that connects two grid points. The capabilities and limitations of the CBAR element are:

- Extensional stiffness along the neutral axis and torsional stiffness about the neutral axis may be defined.
- Bending and transverse shear stiffness can be defined in the two perpendicular directions the CBAR element's axial direction.
- The properties must be constant along the length of the CBAR element. The limitation is not present in the CBEAM element.
- The ends of the CBAR element may be offset from the grid points.
- The effect of out-of-plane cross-sectional warping is neglected. This limitation is not present in the CBEAM element.
- The stress may be computed at up to four locations on the cross section at each end. Additional output may be obtained for intermediate locations along the length of the CBAR using the CBARAO BULK Data entry.
- Transverse shear stiffness along the length of the CBAR can be included.

One of the most difficult aspects of the CBAR (or CBEAM) for the first-time users is understating the need to define an orientation vector. The best way to see the need for the orientation vector is by an example. Consider the two I-beam shown in Figure 13. The I-beams have the same properties because they have the same dimensions, however, since they have specifying the I-beam properties and the location of the end point via the grid points is insufficient, user must also describe the orientation. This is done the orientation vector.

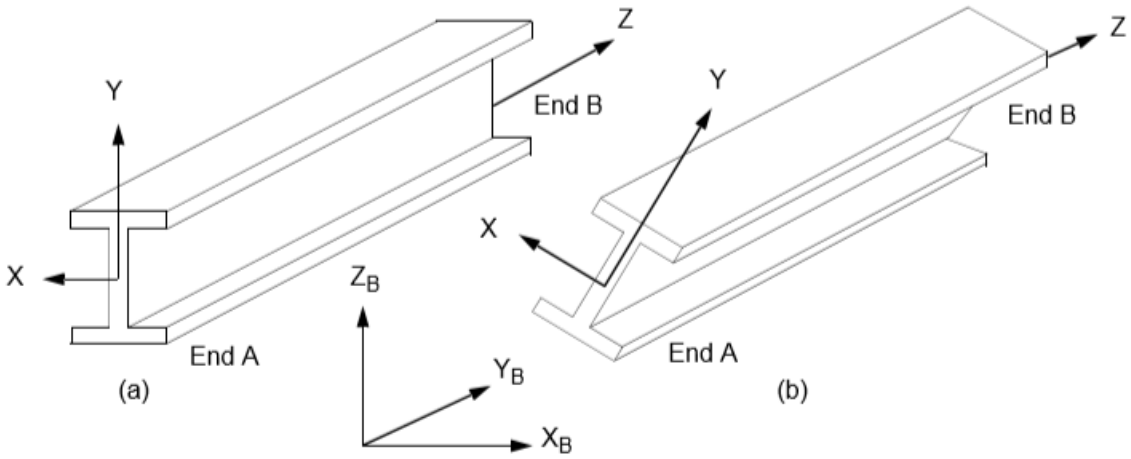

Figure 13. Demonstration of Beam Orientation

Defining the orientation of an element in space is accomplished with the use of an orientation vector. Another way of looking at the orientation vector is that it is a vector that specifies the local element coordinate system. Since the geometric properties are entered in the element coordinate system, this orientation vector specifies the orientation of the element. The orientation vector $\vec{v}$ as it is related to CBAR element coordinate system is shown in Figure 14. Vector $\vec{v}$ defines plane 1, which contains the element x- and y-axes.

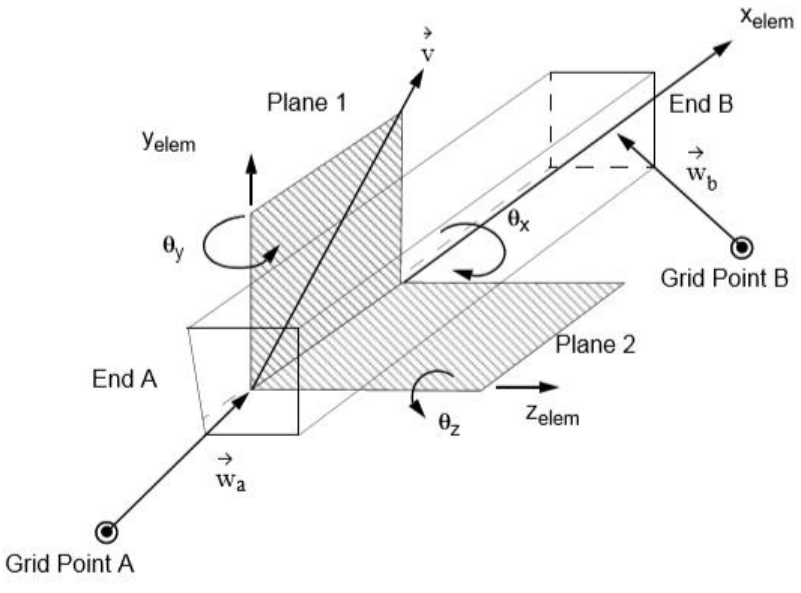

Figure 14. CBAR Element Coordinate System.

Referring to Figure 14, the element x-axis is defined as the line extending from end A (the end at grid point GA) to end B (the end at grid point GB). GA and GB are grid point identification numbers of connection points, they are non-coincident points. From my experience the best way of course is to display full span model, where orientation is visible and user can define whether its correctly defined or not. For the models, because rivets have cross section of rod, for pre-processing user doesn't need much time to think for orientation should be defined, but with different cross section its bit harder. However, for result evaluation it is convenient for user to define user defined coordinate system adequately.

According (Nastran, 2019, pp. 114-115), the CBEAM element provides all of the capabilities of the CBAR element discussed in the above, plus the following additional capabilities:

- Different cross-sectional properties may be defined at both ends and at as many as nine intermediate locations along the length of the beam.
- The neutral axis and shear centre do not need to coincide. The feature is important for unsymmetrical sections.
- The effect of cross-sectional warping on torsional stiffness is included.
- The effect of taper on transverse shear stiffness (shear relief) is included.
- A separate axis for the centre of non-structural mass may be included.
- Distributed torsional mass moment of inertia is included for dynamic analysis.

Because CBEAM has exact same abilities as CBAR and even more, for the paper's models for rivet representation, CBEAM element will be used, to compare it with CBUSH element.

4.3. RBE elements

According [7] (Nastran, 2019, pp. 312-325) an R-type element is an element that imposes fixed constraints between components of motion at the grid points or scalar points to which they are connected. They could also be constraint elements. Thys, an R-type element is mathematically equivalent to one or more multipoint constraint (MPC) equation. Each constraint equation expresses one dependent degree of freedom as a linear function of the independent degrees of freedom. R-type element which will be used in this paper will be RBE2 and RBE3, although, RBE3 element is not rigid element.

RBE2 element is infinitely stiff MPC. This means that the different degrees of freedom connected by RBE2 will behave as if they were part of an infinitely stiff item. This does not mean that the different degrees of freedom (DOF) will have the same displacements (translational and rotational). Only of the nodes connected are coincident the same displacements will be obtained on both nodes for any loading. The RBE2 is an MPC where one single node is defined as independent (providing its 6 translations as independent degrees of freedom) and any degrees of freedom of other nodes are defined as dependent.

Once the geometry is set on the model, the values of the dependent degrees of freedom only depend on the values of the independent degrees of freedom.

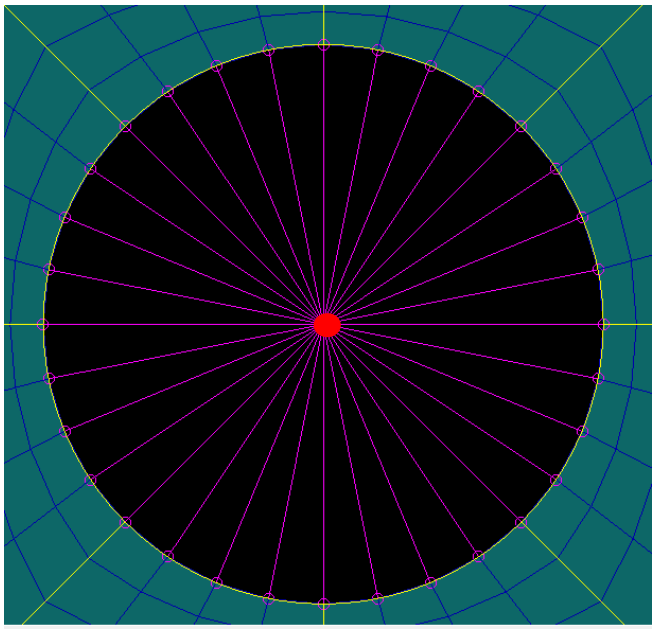

Figure 15. RBE2 element connection.

The RBE2 is normally attached in the following way (Figure 15): the central node in red is the independent one whereas the other nodes are dependent ones (in magenta). The dependent nodes usually connected to some nodes of the FEM and therefore have a stiffness associated for each degree of freedom. If a displacement is enforced on the independent node of the RBE2, the reactions of the structure will depend on the stiffness of the FEM associated with each degree of freedom, but the displacements obtained on the dependent degrees of freedom only depend on the displacements on the independent node. Therefore, the reactions on the MPC depend on the model stiffness but the displacements do not.

The RBE3 element is a powerful tool for distributing applied loads and mass in a model. Unlike RBE2, The RBE3 element has only one dependent node and the others are independent nodes (vice versa for RBE2 element), The RBE3 does not add additional stiffness to the structure. Forces and moments applied to reference points are distributed to a set of independent degrees of freedom based on the RBE3 geometry and local weight factor. The manner in which the forces are distributed is same as to the classical fastener pattern analysis. Consider fastener pattern shown in Figure 16, with a force and moment M acting at reference point A. force and moment can be transferred directly to the weighted center of gravity location along with the moment produced by the force offset. The force distributed to the bolts proportional to the weighting factors. The moment is distributed as forces, which are proportional to their distance from the center of gravity time their weighting factors, as shown in Figure 17. The total force acting on the bolts is equal to the sum of the two forces. These results apply to both in plane and out of plane loadings. Contrary to the RBE2, where the key point is the equation relating the displacements, on the RBE3 the key point is the equation relating the loads. On the RBE3 the loads are calculated distributing the

loading applied on the reference node (dependent degrees of freedom) to the independent degrees of freedom.

In this paper both RBE2 and RBE3 elements will be used to compare how much infinite stiffness affect on rivets load distribution.

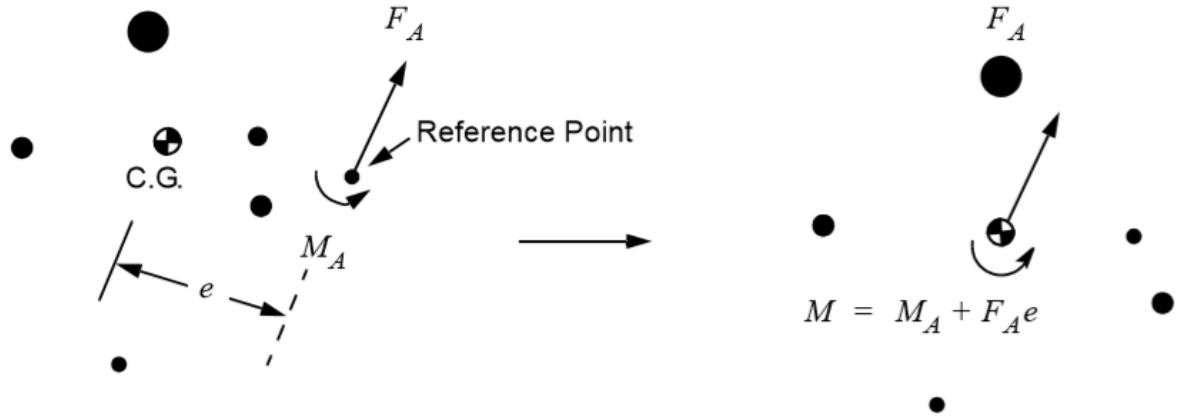

Figure 16 RBE3 Equivalent Force and Moment at the Reference Point

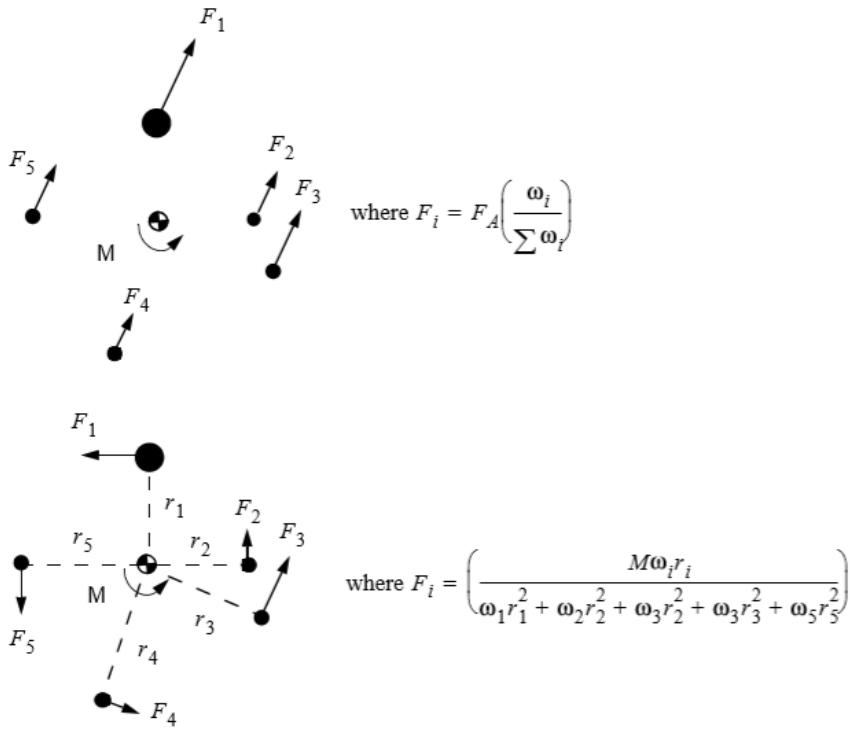

where:

F_i	=	force at DOF i
ω_i	=	weighting factor for DOF i
r_i	=	radius from the weighted center of gravity to point i

Figure 17 RBE3 Force Distribution

4.4. Two-dimensional elements

According [7] (Nastran, 2019, p. 166), MSC Nastran includes two different shell elements (triangular and quadrilateral) and two different stress systems (membrane and bending). There are in all a total of 6 different forms of shell elements. Shell elements differ principally in their shape (Figure 18), number of connected grid points and number of interval stress recovery points. Each element type can be used to model membranes, plates, thick or thin shell. Their properties which are defined using the PSHELL entry, are identical. The important distinction among the elements the elements is the accuracy that is achieved in different applications.

For this paper CQUAD4 (4 means number of nodes) element is chosen, as it's much easier to mesh structures, which are discussed below. One model requires node to node connection, those nodes have to coaxial on x, y or z axis. With CQUAD element it is easy to mesh the structure without extra mesh on mesh.

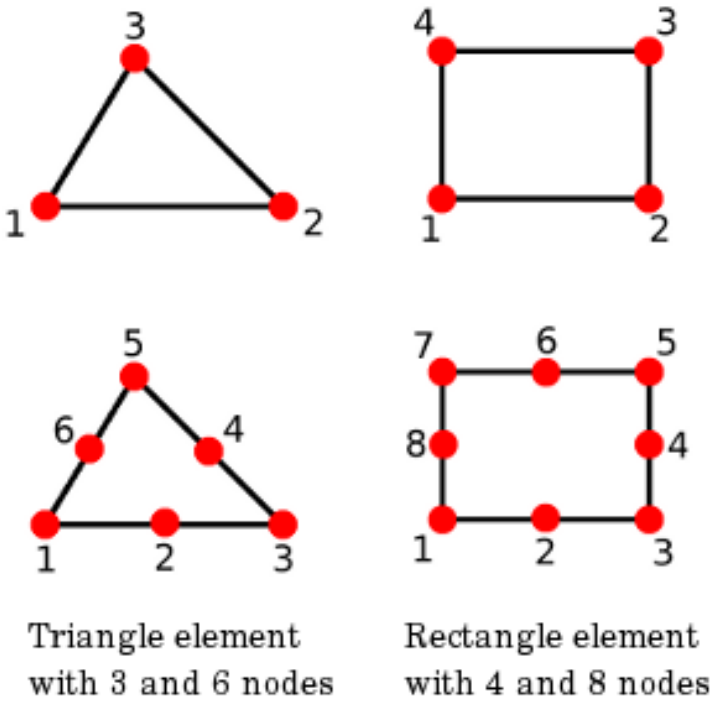

Figure 18. Triangle and Quadrilateral Mesh Elements.

5. Rivet joint analysis

5.1. Three rivets in serial configuration

5.1.1. Traditional approach

In this section will be discussed single row, serial configuration lap rivet joint (Figure 19). Mechanical properties of sheet material 2024-T3 are shown in Table 1. For this experiments AVEX 1691-0512 blind rivets are chosen (Table 2). Geometries are shown in Figure 50. As was mentioned above, in this case load distribution is not uniform. Table 3 shows rivet concentration factor in different number of rivets.

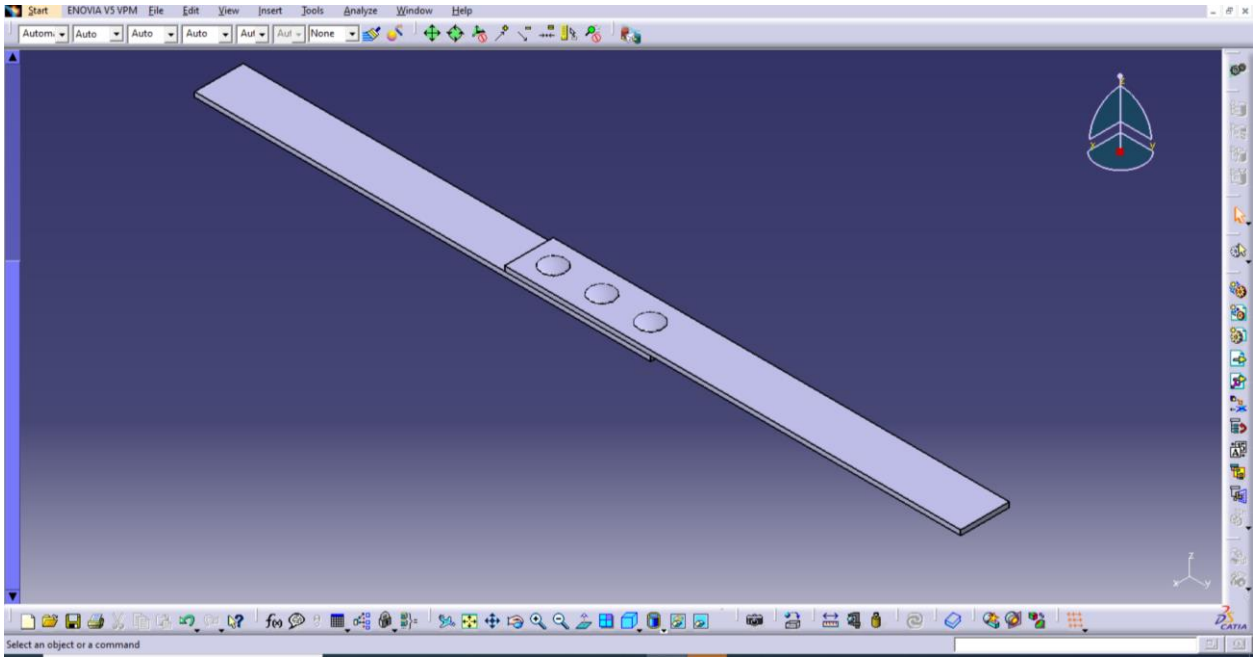

Figure 19. Three Rivets in Serial. Lap Joint.

2024-T3	
Ultimate tesnion strength [Mpa]	441
Yield tension strength [Mpa]	324
Ultimate bearing strength [Mpa]	889
Yield bearing strength [Mpa]	607
Ultimate shear strength [Mpa]	269
Young mudulus E [Mpa]	72395
Poisson ratio [-]	0.33
Shear Modulus [Mpa]	269

Table 1. Mechanical properties of 2024-T3.

Rivet type	Diameter [mm]	Coverage S [mm]	Head diameter D [mm]	K [mm]	Recommended hole [mm]	min. shear load [N]	min. tensile load [N]
1691-0512	4	1.2 to 6.3	8	1.4	4.1-4.3	1000	1555

Table 2. Properties of AVEX blind rivet.

To obtain rivet shear failure, it is necessary to have rivet strength, less than sheet strength, for that next calculations must be made:

1. Calculate shear, bearing and tension forces for sheet to compare minimum sheet failure load to rivet strength. Sheet properties are shown in Table 1.

Ultimate tension force $F_t = A_t\sigma_t = 441 * 30.48 = 13449.73$ [N] where $A_t = (p - D)t = 30.48\ [mm2]$ and σ_t-sheets Ultimate tension strength p-pitch 16mm, D-rivet diameter 4mm, t-sheet thickness.

Ultimate bearing force $F_b = A_b\sigma_b = 10.16 * 889 = 9036.55$ [N] where $A_b = Dt = 10.16$ [mm2] and σ_b-sheets Ultimate bearing strength.

Ultimate shear force $F_{ms} = A_{ms}\sigma_s = 40.64 * 269 = 10927.93$ [N] where $A_{ms} = mt = 40.64$ [mm2] and σ_b-sheets Ultimate shear strength, m-length between edge and center of rivet 8mm.

Minimum force for sheet failure is F_b, so we can compare max rivet load (F_r) to this force.

2. Compare sheet minimum strength (from calculation it's bearing stress) to rivet:
   According [3] (Dimarogonas, 2001, pp. 512-513) Table 3, load distribution between rivets should be:
   $F_{b_{1,3}} = \frac{K_t F_b}{n} = \frac{1.059*9036.55}{3} = 3189.90\ [N]$ 35% of total load
   $F_{b_2} = \frac{(n-2K_t)F_b}{n} = \frac{0.882*9036.55}{3} = 2656.75\ [N]$ 30% of total load

RF $= \frac{F_{r_{1,3}}}{F_{b_{1,3}}} = 0.31$, RF $= \frac{F_{r_2}}{F_{b_2}} = 0.38$, only rivets will fail.

No. of rivets	1	2	3	4	5	6
Concentration factor K_t	1	1	1.059	1.16	1.3	1.44

Table 3. concentration factors in different number of rivets in serial configuration According [3] (Dimarogonas, 2001, pp. 512-513)

5.1.2. Finite element models

According to [2] (Niu, 1988, p. 236) ratio between plate/sheet and rivet constants defines load distribution on rivets. (Figure 20). According [8] (Software, 2018, p. 2721) rivet spring constants are calculated with formulas:

$KT_1 = \frac{EA}{L}$, $KT_2 = \frac{G_2 A_s}{L}$, $KT_3 = \frac{G_3 A_s}{L}$,

$KR_1 = \frac{GJ}{L}$, $KR_2 = \frac{G_2 A_s L}{3} + \frac{EI}{L}$, $KR_3 = \frac{G_3 A_s L}{3} + \frac{EI}{L}$, where A-rivet cross section area $\frac{\pi D^2}{4}$, L length of middle plane of sheets, $A_s = \frac{3A}{4}$, $I = \frac{\pi D^4}{64}$ second moment of inertia, $J = \frac{\pi D^4}{32}$ - polar moment of inertia, E-young modulus and G shear modulus. inputs and results of rivet spring constants are shown in Table 4, because rivet is made from isotropic material G2=G3=G.

Sheet constant: $K = \frac{AE}{l} = \frac{40.64*72395}{16} = 183883.3\ \frac{N}{mm}$ where A is sheet cross section area, E-young modulus, l-rivet pitch length.

Because, rivets have only shear force applied, ration (n) between structure member constants will be: $n = \frac{K}{KT_{2,3}} = 0.54$. with these calculations, forces in the first and last rivet in my FEM results should be approximately between 36-38% of total force, while middle rivet takes approximately 24-28% of total load.

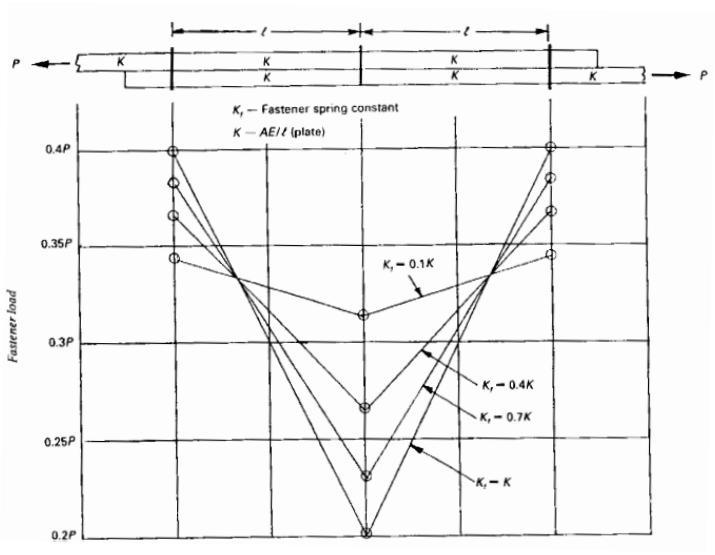

Figure 20. Three Rivets in Serial, FE analysis according [2] (Niu, 1988, p. 236)

In the first two joint models for sheet description, 2D shell QUAD4 elements are used with 2mm of element length, on sheet geometry rivet holes were also applied, for rivet – at first analysis CBUSH elements. The properties of CBUSH elements are shown in Table 4. element orientation is <1 0 0>, at second analysis CBEAM elements, property for that element is: circular cross section with radius of 2mm element orientation same as CBUSH. At the first attempt rivet and sheet are connected with RBE2 element (Figure 21), on second try with RBE3. Model is fixed at one and in every translational and rotational direction, while the other end, where force is applied, is fixed in every direction except one translational way which is parallel to the force vector. For the uniform load distribution along the sheet cross section, the node, where load is applied, is connected with surrounding nodes with the RBE2 element (Figure 22). whole model is shown in Figure 65. Analysis is performed with 4 load cases: 1000, 2000, 3000, 4000 newtons. Analysis is done with 106 nonlinear solution.

D [mm]	4
E [MPa]	71000
G [MPa]	26691.73
A [mm2]	12.57
As=3A/4 [mm2]	9.42
L [mm]	2.54
I [mm4]	12.57
J [mm4]	25.13
KT1 [Nmm-1]	351264.69
KT2 [Nmm-1]	99040.80
KT3 [Nmm-1]	99040.80
KR1 [Nmm]	264108.79
KR2 [Nmm]	564255.22
KR3 [Nmm]	564255.22

Table 4. Spring constants

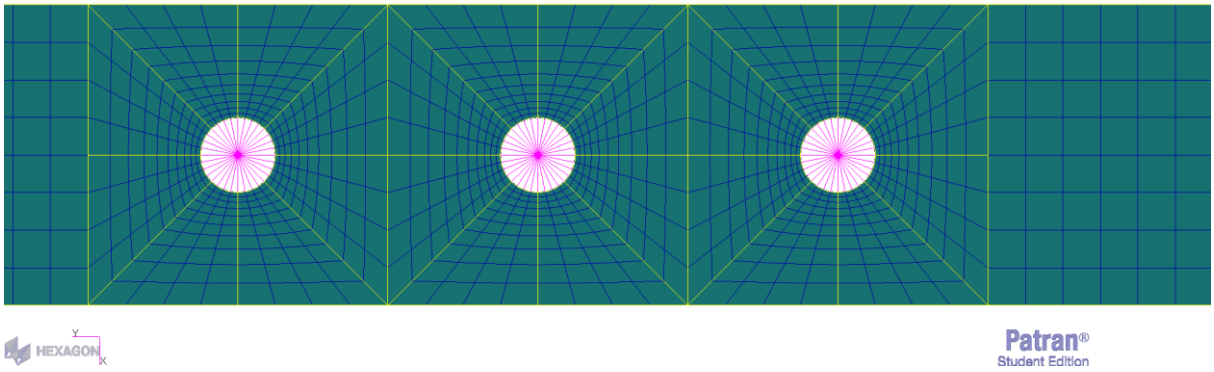

Figure 21. Rivet-Sheet Elements Connection with RBE2/RBE3 elements (pink element- RBE).

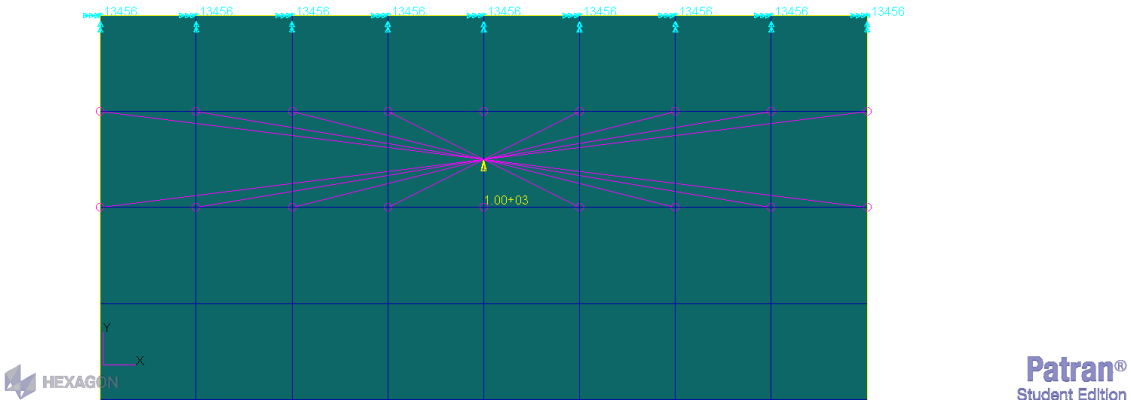

Figure 22. Applied force on the model.

The result comparison of those models are shown in Figure 23 and Figure 24. As shown in the outcome figures, difference between both models are very small (less than 1%). If the analysis aim is only to find load distribution on rivets both RBE2 and RBE3 element is good, if there also need to find stress distribution on holes then due to infinite stiffness RBE2 element is not good choice, Figure 61 and Figure 62. As this paper aims only rivet failure, stress distribution on holes will be discussed with traditional approach and FEM results. Peak of stress around hole can be calculated with formula: $\sigma_{avg} = \frac{F}{(p-d)t} = \frac{1000}{(16-4)2.54} = 32.8\ MPa, \sigma_{max} = k_t\,\sigma_{crit} = 2.425 * 32.8 = 79.54\ MPa,$ where $k_t = 2.425$ is stress concentration factor which can be found in Figure 60. FEM results show that model where RBE2 elements are used stress difference is 28.6%, while on the other 5.6%, on the first model big difference might be caused by “infinite” stiffness provided by rigid body element.

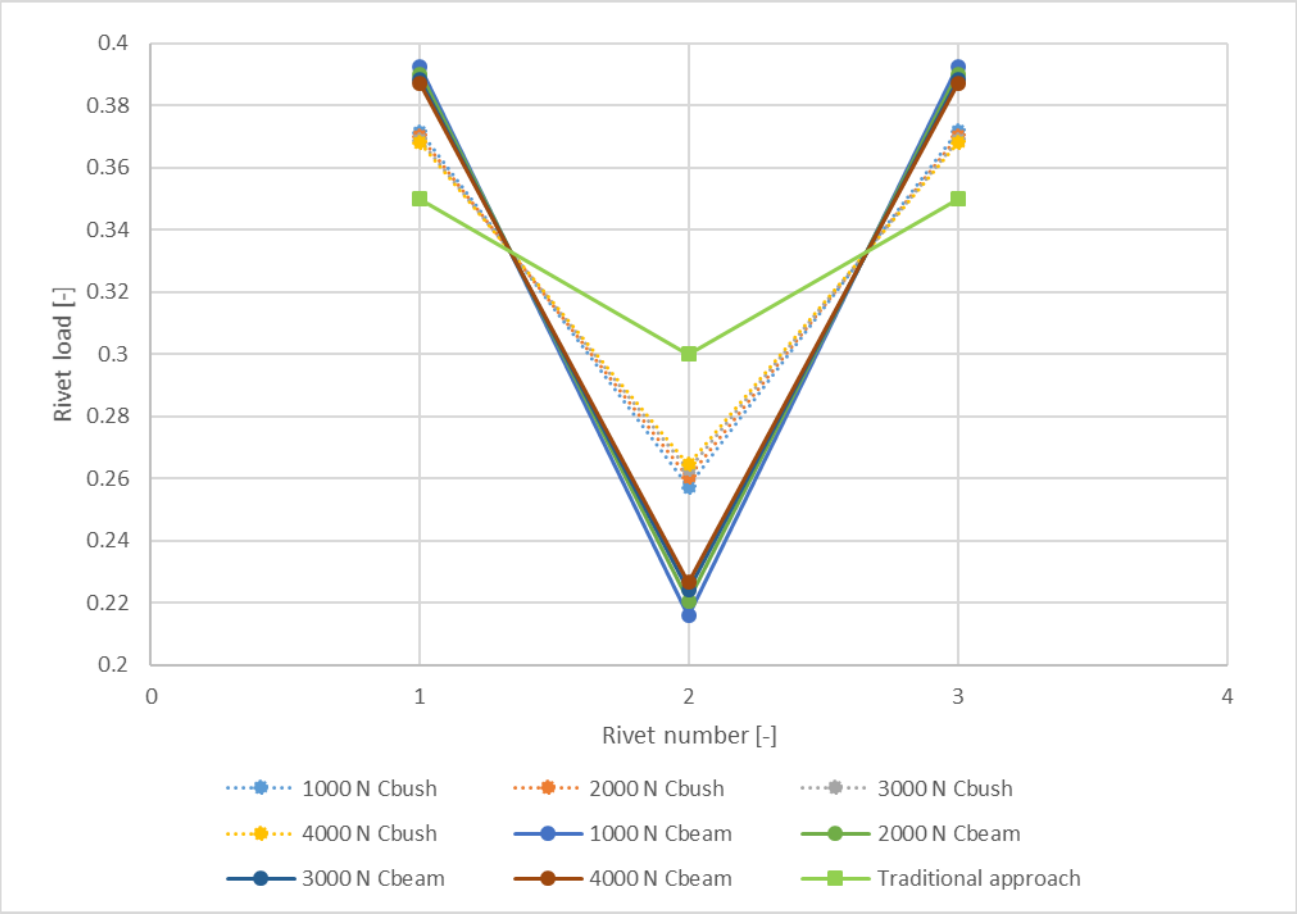

Figure 23. FEM results with RBE2 elements (N-applied force in newton)

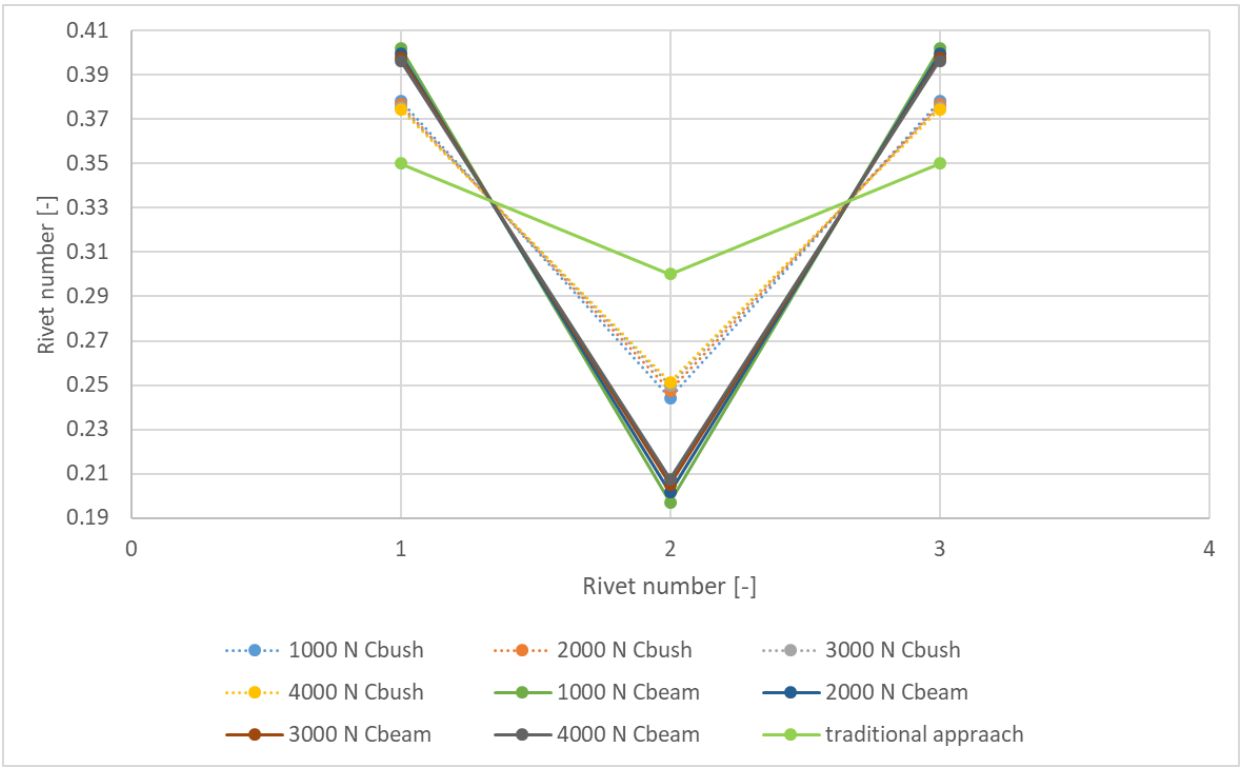

Figure 24. FEM results with RBE3 elements (N-applied force in newton)

Second two models were made with same elements but without rivet holes, which takes some time, as apart from making geometry, correct meshing time around holes is also increased, also as mentioned above this paper is oriented on rivet shear failure. In the model RBE elements are also used as rivet to sheet element connection (Figure 25). Results for RBE3 elements are shown in Figure 26 and for RBE2 - Figure 27. As shown from these results, maximum difference between these models and traditional approach and Nius' FE model is in the model where RBE2 elements are used, comparison with "hand calculation" up to 6%, with Niu - 2-3%.

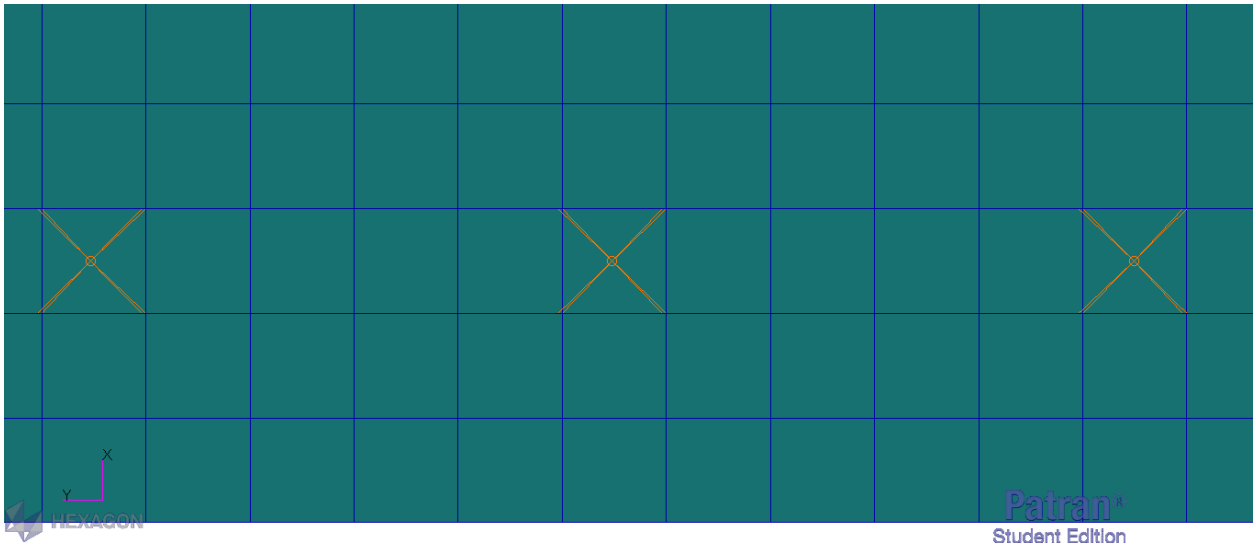

Figure 25. Rivet-Sheet connection without rivet holes in the model.

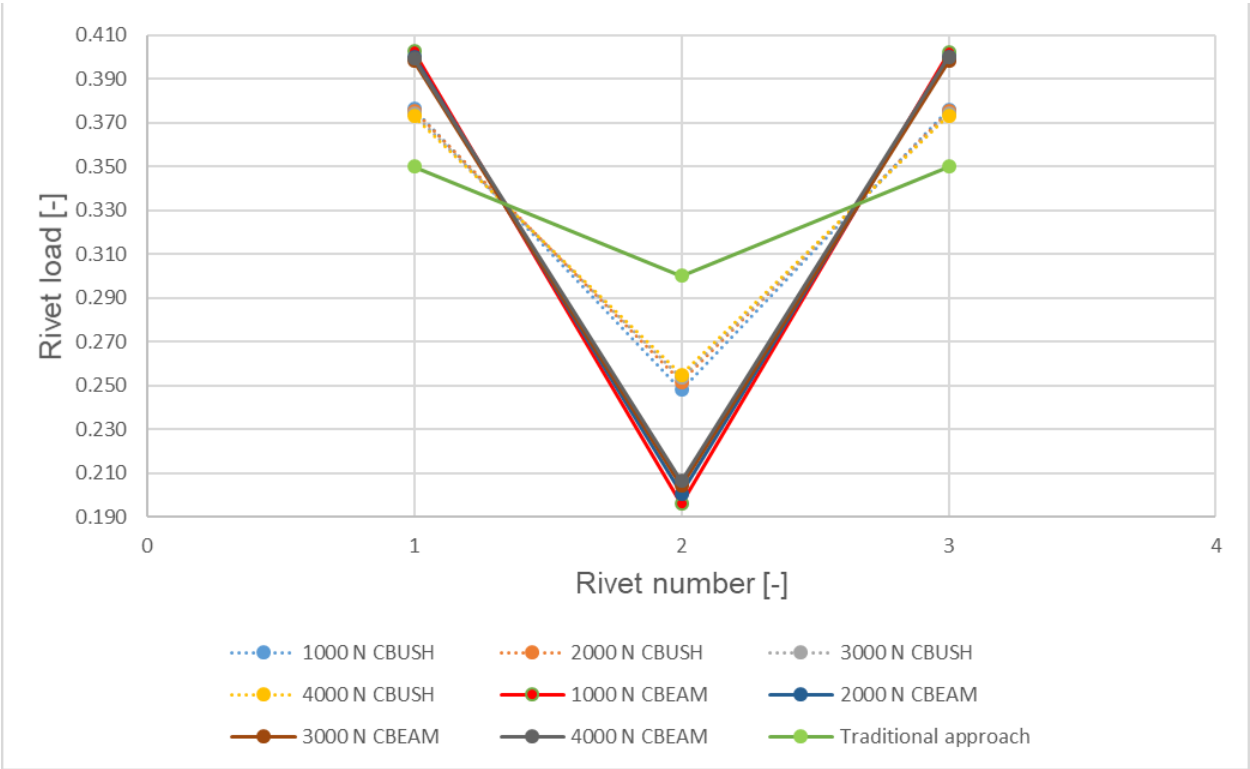

Figure 26. FEM results, with different load cases (N-newton, model with RBE3 elements).

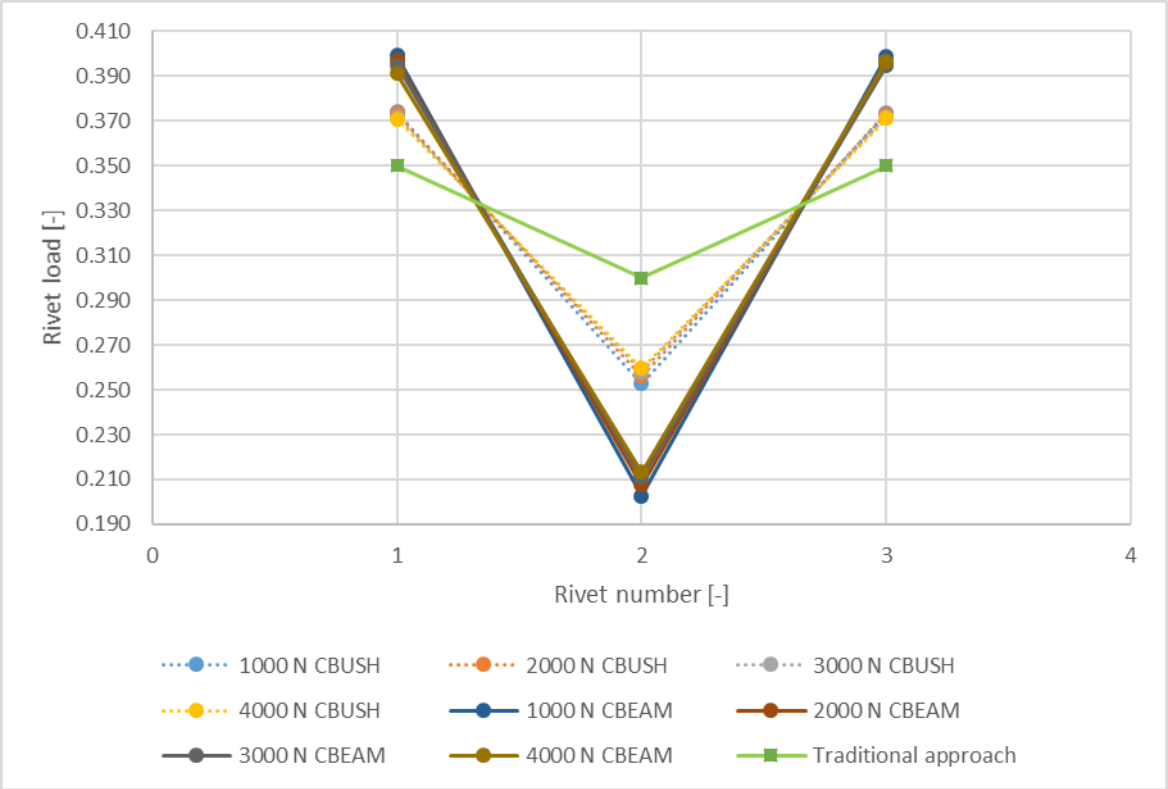

Figure 27. FEM results, with different load cases (N-newton, model with RBE2 elements).

In the final model, same elements are used. Rivet and sheet elements are connected directly node to node (Figure 28), without any additional MPC elements, results of that analysis are shown in Figure 29.

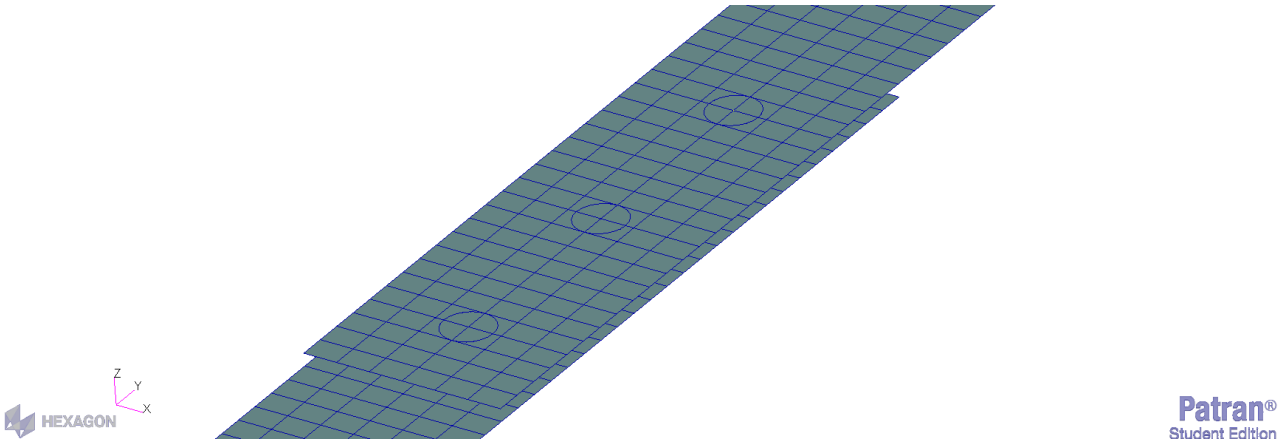

Figure 28. Node to node Connection

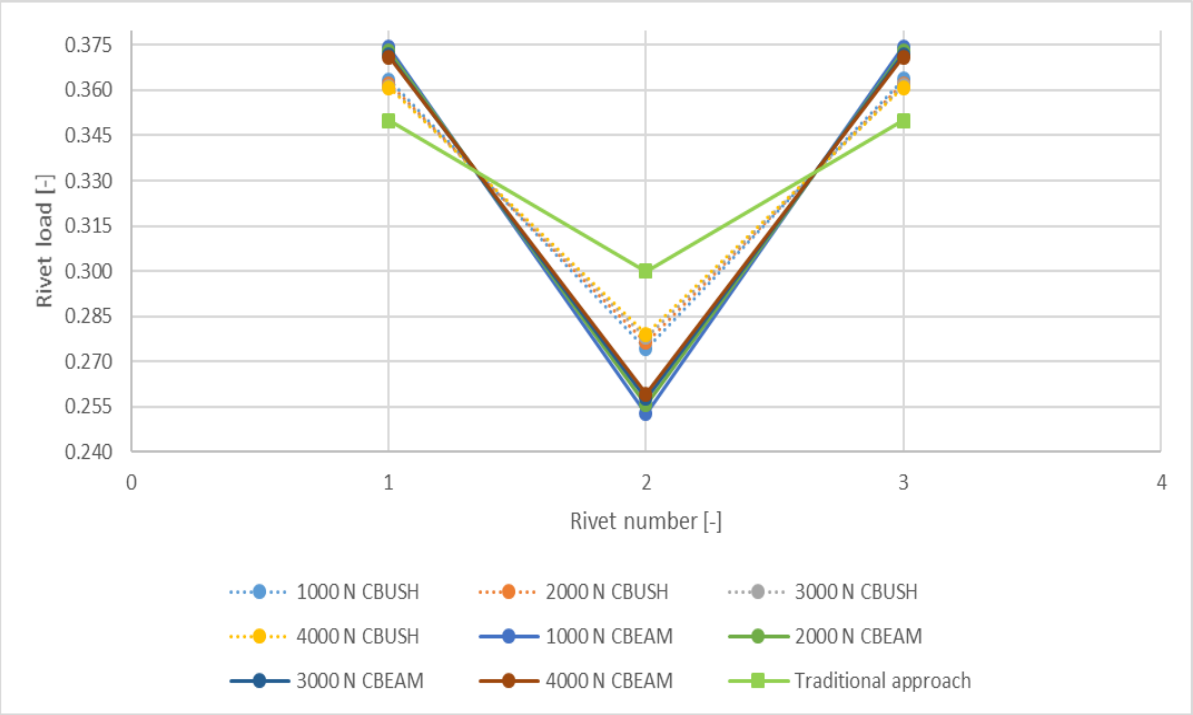

Figure 29. FEM results of node to node connection (N-applied force in newton).

As shown from result figures above, it can be said that joints with rivet holes in them is quite accurate in stress distribution on holes compare with traditional calculation, RBE3 element is used to link rivet element with sheet element, but because this paper is oriented on rivet shear failure, main concern will be load distribution to detect minimum load, under which, according supplier, rivet can withstand. From the figures it can be said that the holes on geometry doesn't have much influence on load distribution and difference is less than 1% on both elements (CBUSH CBEAM), more influence has RBE elements, which is also not bigger than 1%, because of that all models can be considered sufficient. But the best model I believe is the last model, the simplest one "node to node" connection, with CBUSH element as a rivet. Not only it is more accurate (not too great 1-2% different values from traditional calculation than other models), but also it takes less time to model, user doesn't need to use any extra element for rivet to sheet connection and to think their input properties. Reason for that I think is that program doesn't need to consider those extra codes for extra elements and also error for stiffness transfer is also neglected. Reason why CBEAM and CBUSH elements results has different values, is there dependence on elements length in model, as was mentioned above CBUSH element is scalar element, where user inputs its stiffness, on the other hand in CBEAM element user defines only cross sectional etc. but element also depends element length in model. For example, user can make 5mm length element and if he/she will input element stiffness with 1mm length in CBUSH, whole element will have stiffness considering length of 1mm. while in CBEAM element stiffness will be depending real model element length.

5.2. Three rivets in parallel configuration

5.2.1 Traditional approach

In this section will be discussed single row, parallel configuration lap rivet joint (Figure 30). mechanical properties of sheet material 2024-T3 are shown in Table 1. Dimensions of structure are shown in Figure 53. For this experiments AVEX 1691-0512 blind rivets are chosen (Table 2). As mention above in this case load distribution is uniform.

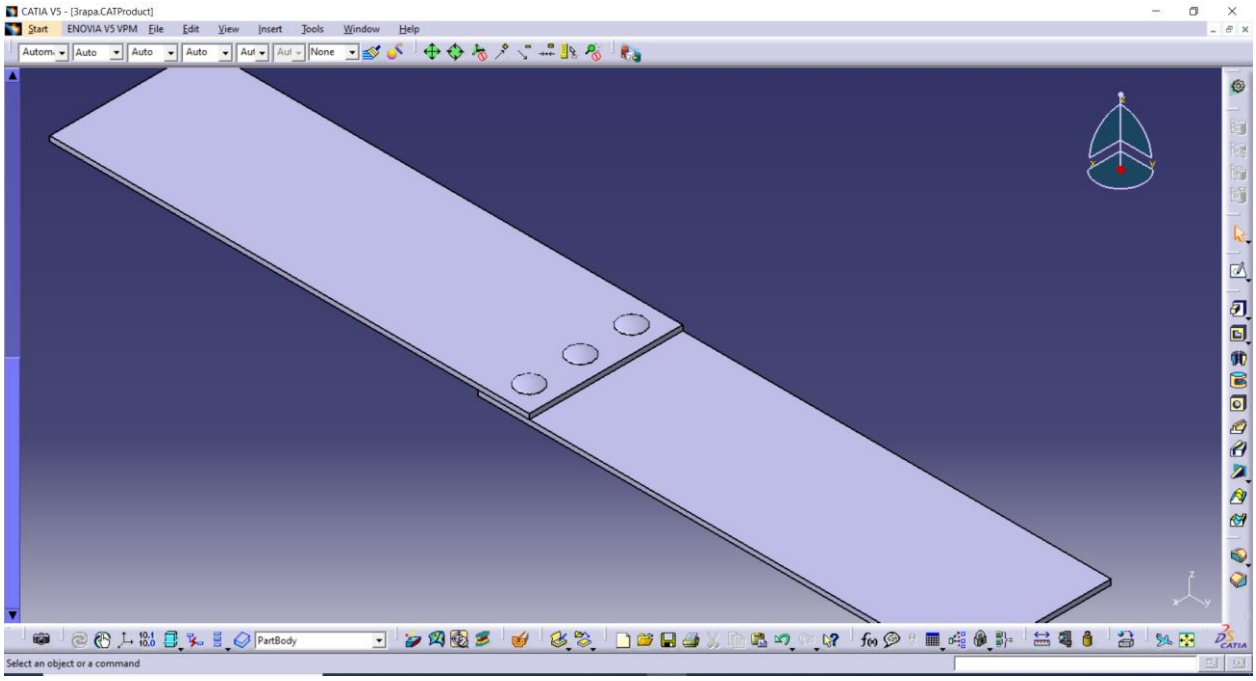

Figure 30. Three rivets in parallel, lap joint.

To obtain rivet shear failure, it is necessary to have rivet strength less than sheet strength, for that next calculations must be made:

1. Calculate shear, bearing and tension forces for sheet to compare minimum sheet failure load to rivet strength. Sheet properties are shown in Table 1.
   Ultimate tension force $F_t = A_t\sigma_t = 40349.18$ [N] where $A_t = 3(p-D)t = 91.44$ [mm2] and σ_t-sheets Ultimate tension strength p-pitch 16mm, D-rivet diameter 4mm, t-sheet thickness.
   Ultimate bearing force $F_b = A_b\sigma_b = 27109.64$ [N] where $A_b = 3Dt = 30.48$ [$mm2$] and σ_b-sheets Ultimate bearing strength.
   Ultimate shear force $F_{ms} = A_{ms}\sigma_s = 32783.80$ [N] where $A_{ms} = 3mt = 121.92$ [mm2] and σ_b-sheets Ultimate shear strength, m-length between edge and center of rivet 8mm.

Minimum force for sheet failure is F_b, so we can compare max rivet load (F_r) to this force.

2. Compare sheet strength to rivet:
   According to traditional analysis, which corresponds traditional calculation, load distribution between rivets will be approximately equal: $F_{b_{1-3}} = 0.33F_b$

RF $= \frac{F_{r_{1-3}}}{F_{b_{1-3}}} = 0.11$, only rivets will fail.

5.2.2 Finite element models

In the first two joint models for sheet description, 2D shell QUAD4 elements are used, on sheet geometry rivet holes were also applied, for rivet – at first analysis, the CBUSH elements, properties are shown in Table 4 element orientation is <1 0 0>, at the second analysis the CBEAM elements, property for that element is: rod cross section with the radius of 2mm element orientation <1 0 0>. At the first attempt rivets and sheets are connected with the RBE2 element (Figure 31), on the second try with the RBE3. Model is fixed at one end in every translational and rotational direction, while the other end, where the force is applied, is fixed in every direction except one translational way which is parallel to the force vector. For the uniform load distribution along sheet cross section, node, where the load is applied, is connected with surrounding nodes with the RBE2 element (Figure 32). whole model is shown in Figure 66. The force itself is static, the analysis is performed with 4 load cases, which are 1000, 2000, 3000, 4000 newtons. Analysis is done with 106 nonlinear solution, due to rivet/sheet connection.

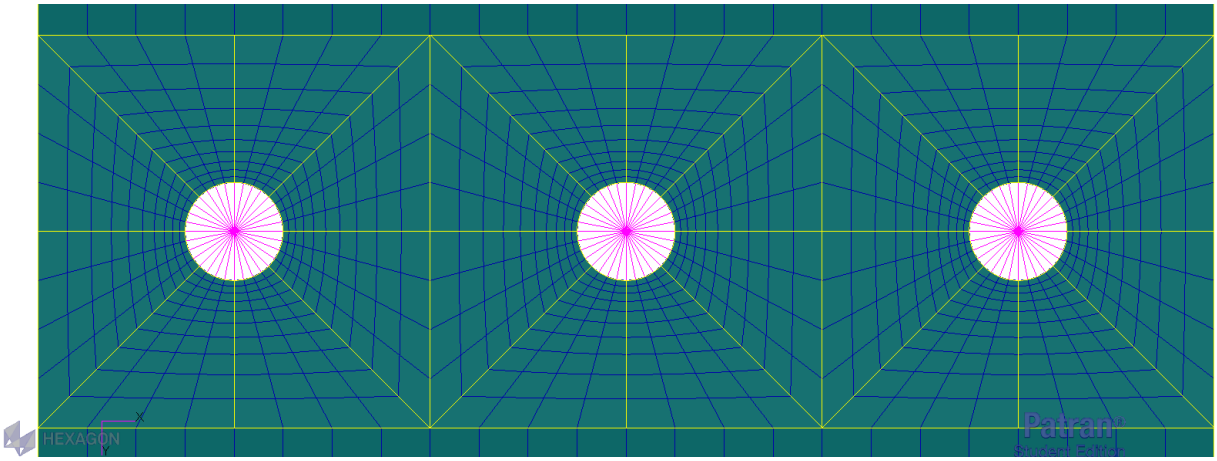

Figure 31. FE model with rivet holes

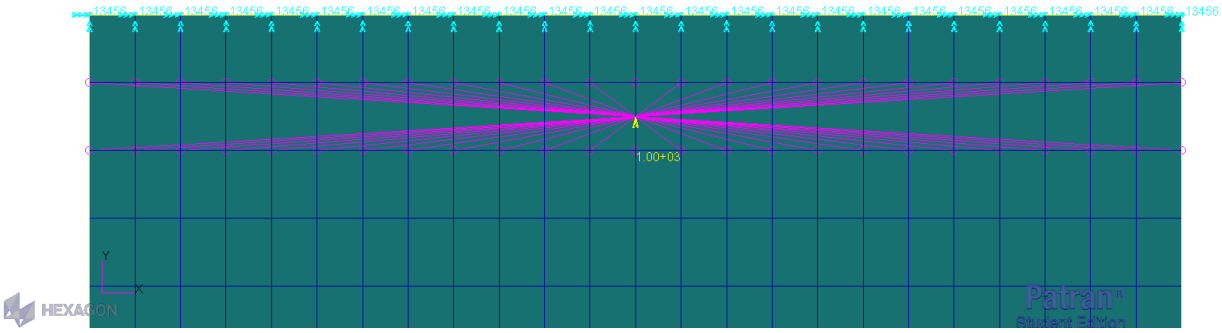

Figure 32. Applied force on the model.

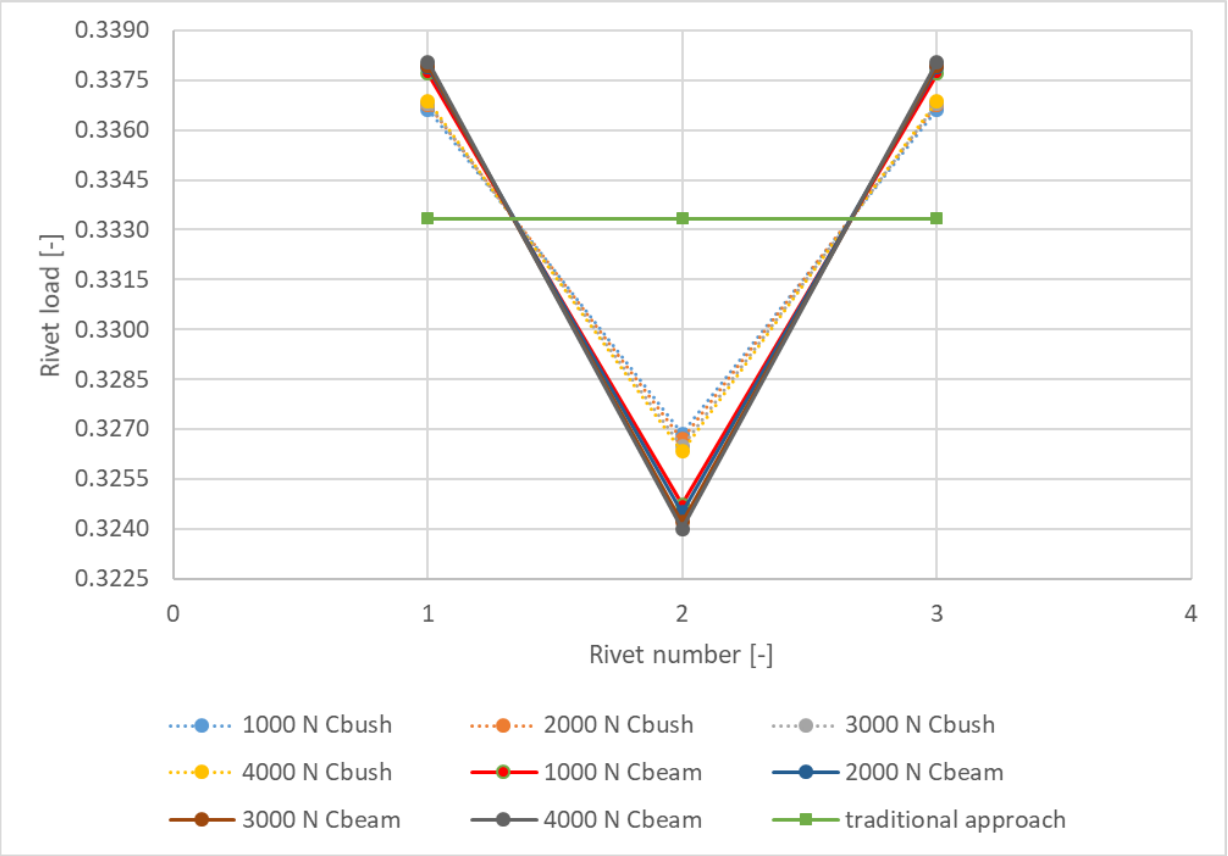

Figure 33. FEM results with RBE3 and with rivet holes in the model.

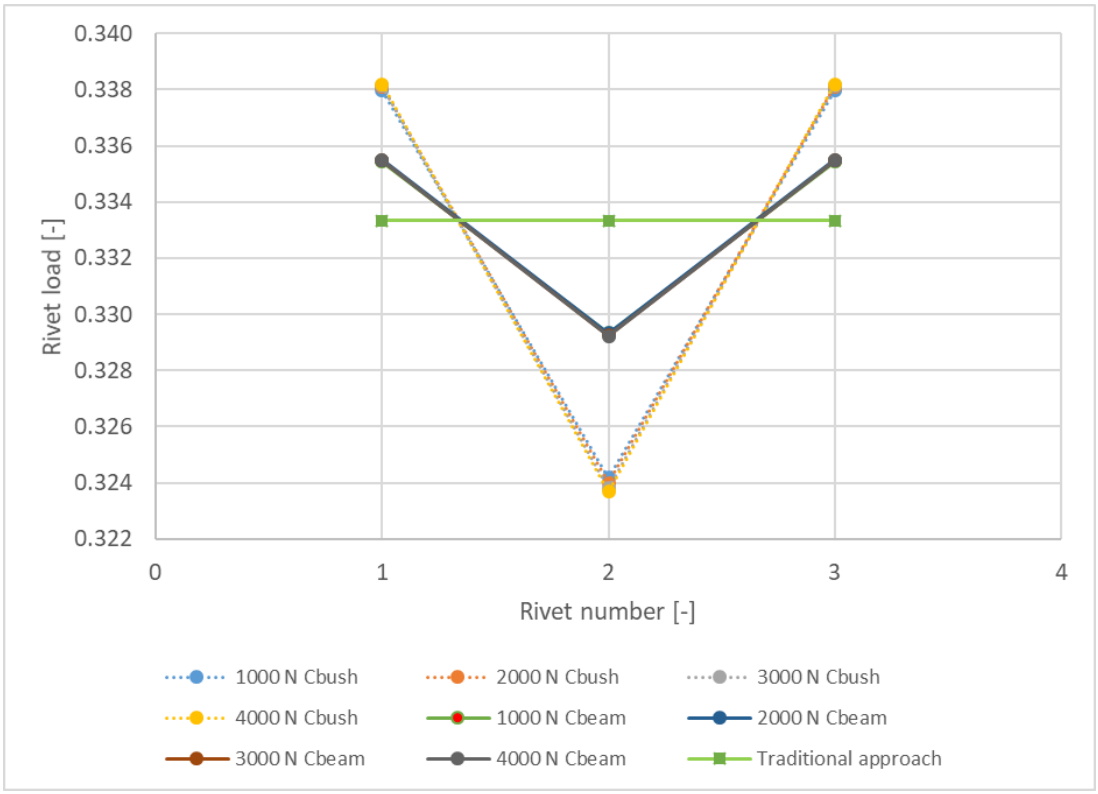

Figure 34. FEM results with RBE2 and with rivet holes in the model.

Result comparison of those models are shown in Figure 33 and Figure 34. As shown in the outcome figures, both model results are quite the same which means there is very small effect on rivet load distribution whether the RBE2 or the RBE3 element is used, but because the difference is not great, less than 1%, the model can be considered as sufficient, if the analysis aim is only to find the load distribution on the rivets, if there's also need to be found stress distribution on the holes then due to infinite stiffness this type of model is not good choice, Figure 63 and Figure 64. As this paper aims only rivet failure, stress distribution on the holes will be discussed with traditional approach and the FEM results. Peak of stress around hole under 1000 newton load can be calculated with formula: $\sigma_{avg} = \frac{F_r}{3(p-d)t} = \frac{1000}{3(16-4)2.54} = 10.93\ MPa, \sigma_{max} = k_t\,\sigma_{avg} = 2.425 * 10.93 = 26.5\ MPa$, where $k_t = 2.425$ is stress concentration factor which can be found in Figure 60. FEM results show that model was RBE2 elements is used stress difference is 37.36%, while on the other 21.13%, on the first model big difference might be caused by "infinite" stiffness provided by rigid body element.

In the second model same elements, properties and geometry are used, except in the sheet geometry rivet holes are not considered (Figure 35). Results are shown if Figure 36 and Figure 37.

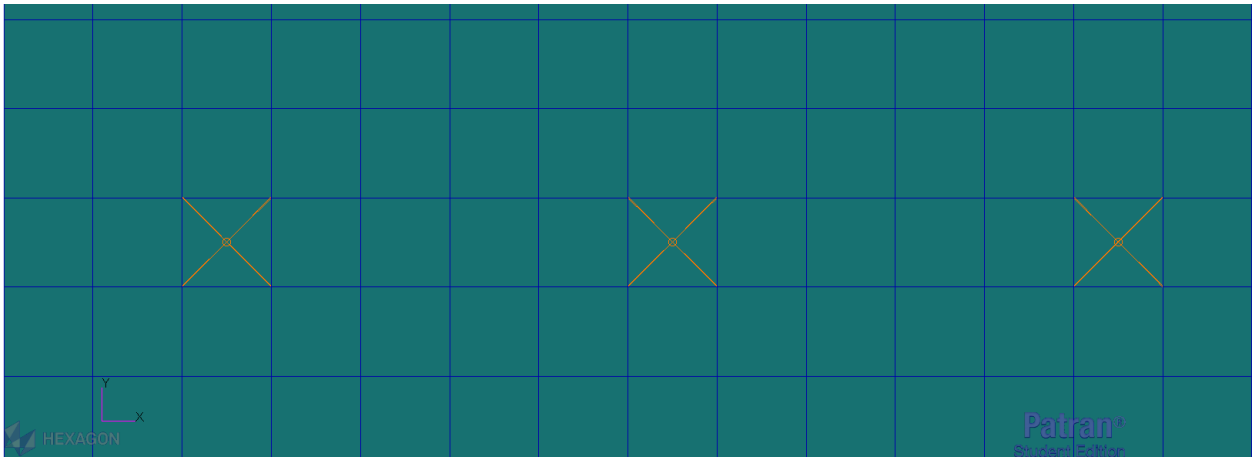

Figure 35. FE model without rivet holes in the model

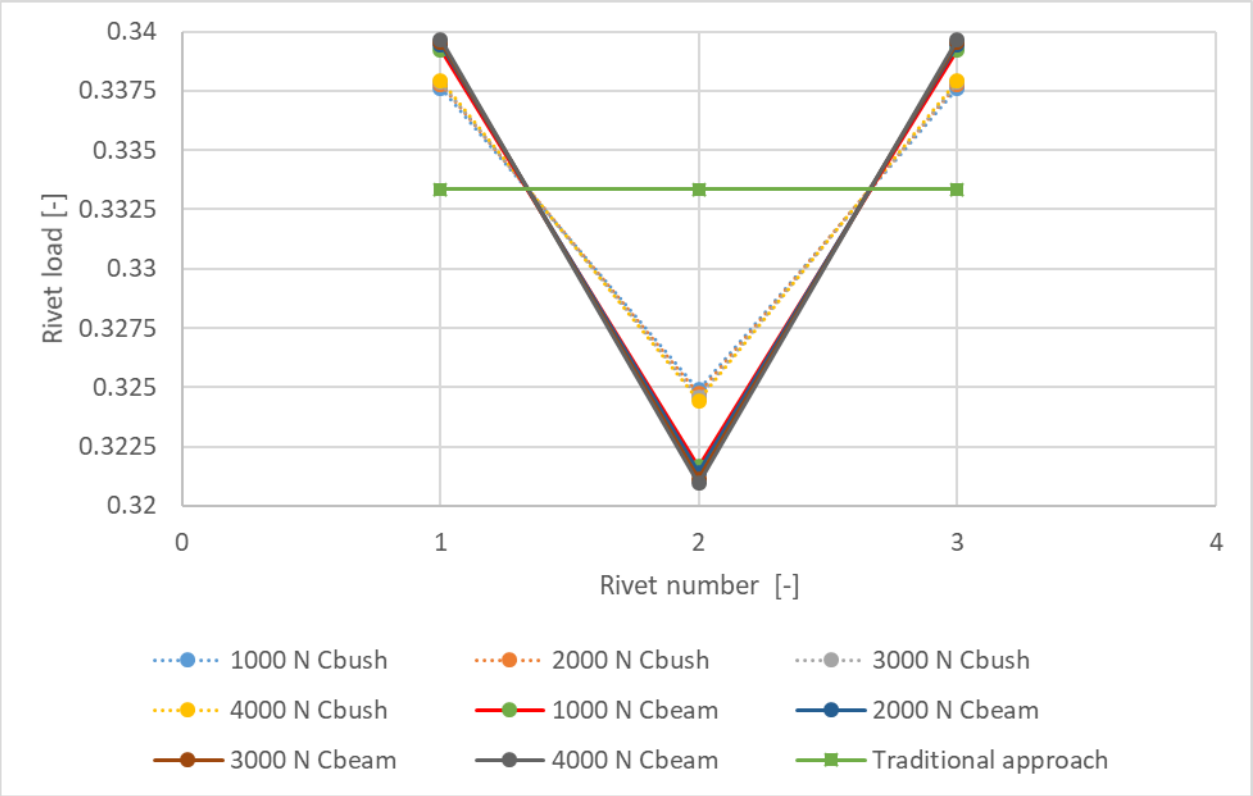

Figure 36. FEM results with RBE3 and without rivet holes in the model (N-applied force in newtons).

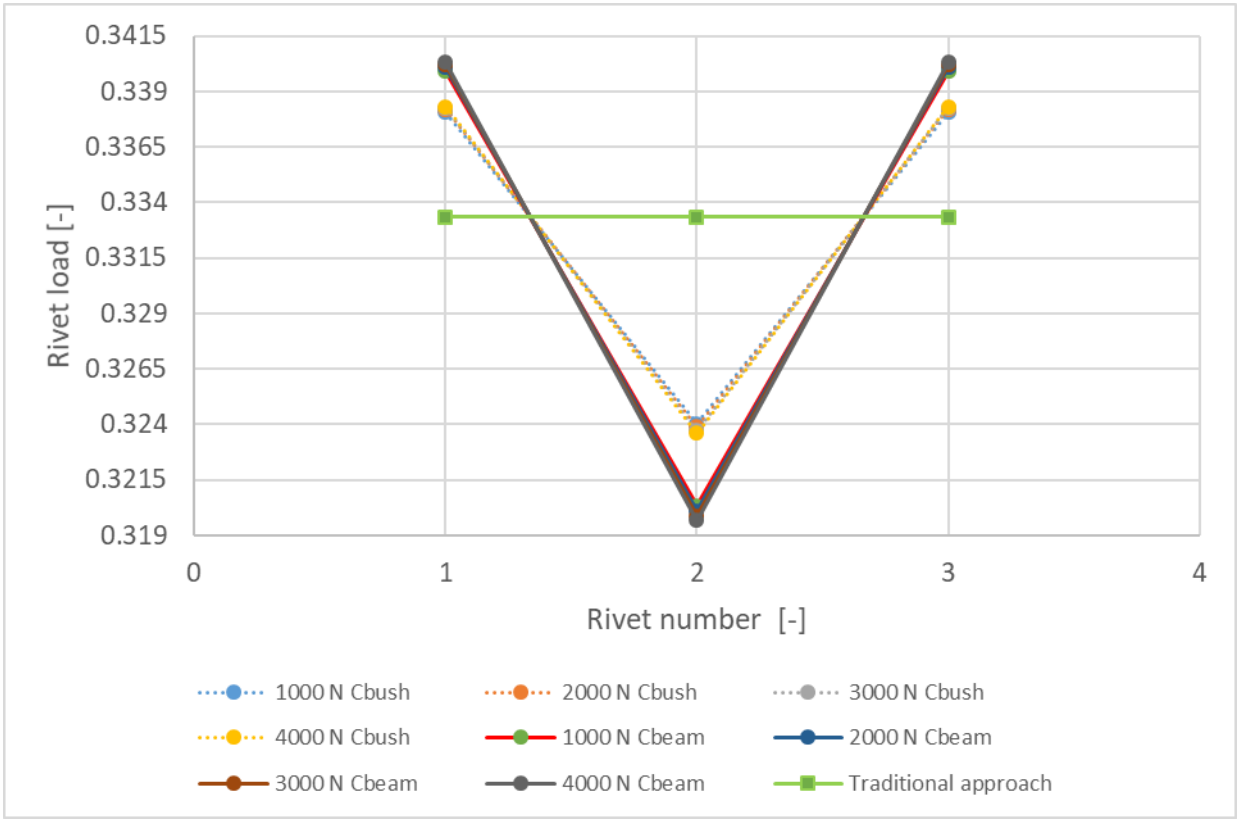

Figure 37. FEM results with RBE2 and without rivet holes in the model (N-applied force in newtons).

The last model MPC elements were neglected and the rivet to sheet connection is node to node as shown in Figure 38. Results are shown in Figure 39.

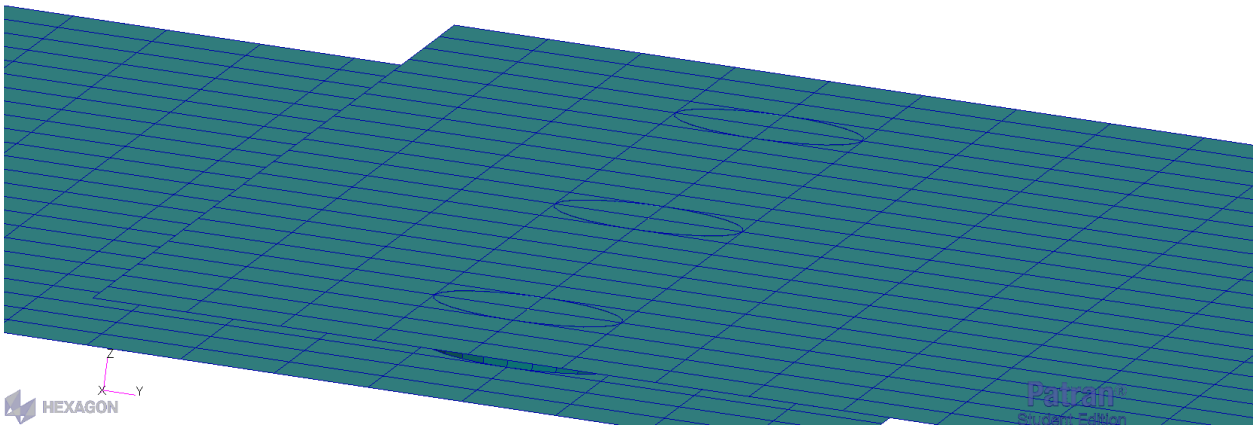

Figure 38. Node to node connection

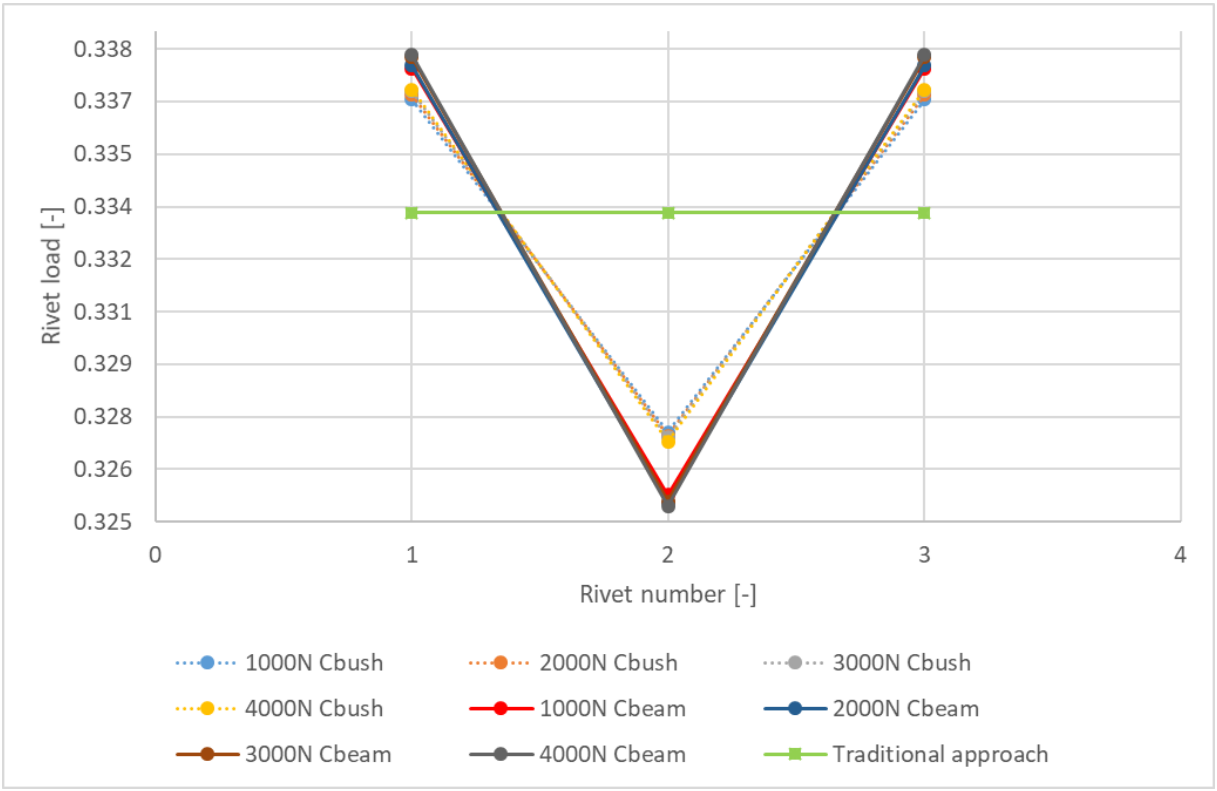

Figure 39. FEM results of node to node connection model

In this configuration difference in every case is less than 1%, that's why main criteria to choose which model is better than the others, is simplicity, where again "node to node" connection is the best option with CBUSH element.

5.3. Eccentric configuration

In this section single row lap rivet joint only rivet shear failure will be discussed (Figure 40). Sheet material mechanical properties are shown in Table 5. The geometric dimensions are shown in Figure 56. In this experiments AVEX blind rivet 1691-0512 is chosen, properties are shown in Table 2.

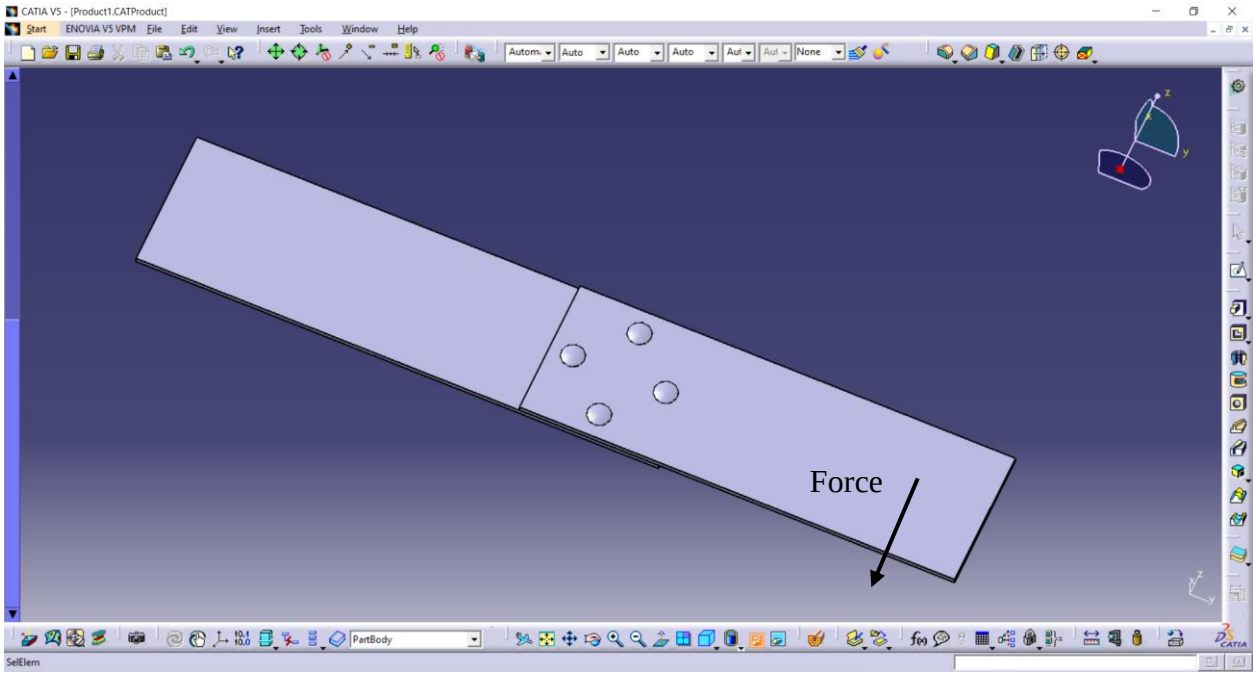

Figure 40. Eccentric configuration

5.3.1. Traditional approach

For the traditional calculation rivet joint is assumed to be perfectly rigid. To obtain rivet shear failure, it is necessary to have rivet strength less than sheet strength, for that next calculations must be made:

1) Primary and secondary force calculation:

Primary force due input shear force in each rivet: because we have 4 rivet total load will be divided to 4. $F_{p.n} = \frac{F}{4}$. Secondary load: center of shear: $X_{c.s} = \frac{\sum X\ G\ A}{\sum G\ A} = 114\ mm : Y_{c.s} = \frac{\sum Y\ G\ A}{\sum G\ A} = 0\ mm,$ where: X - rivets x position from center of load [mm] G-shear modulus [MPa] A-area of rivet [mm2] Y-rivets y position from center of load [mm] length between C.S and center of rivet: $r = \sqrt{x'^2 + y'^2}$ where x' and y' are horizontal and vertical length between rivet center and C.S. Secondary load due to bending moment: $F_{s.n} = Fl\frac{rGA}{\sum r^2 GA}$ where: F - total load [N] l - length between C.S and load center $l = \sqrt{{X_{c.s}}^2 + {Y_{c.s}}^2} = 114$ [mm] r -length between C.S and center of rivet [mm]. Calculation results are shown in Table 6, force vectors in Figure 41.

AISI 8630	
Ultimate tesnion strength [Mpa]	620.5
Yield tension strength [Mpa]	482.6
Ultimate bearing strength [Mpa]	1310.0
Yield bearing strength [Mpa]	827.4
Ultimate shear strength [Mpa]	372.3
Young mudulus E [Mpa]	199948.0
Poisson ratio [-]	0.32
Shear Modulus [Mpa]	75842.3

Table 5. Mechanical properties of AISI 8630.

Rivet number	1	2	3	4	∑
x [mm]	130.00	114.00	98.00	114.00	
y [mm]	0.00	16.00	0.00	-16.00	
A [mm2]	12.57	12.57	12.57	12.57	50.27
XA [mm3]	1633.63	1432.57	1231.50	1432.57	5730.27
YA [mm3]	0.00	201.06	0.00	-201.06	0.00
GA [N]	335418.16	335418.16	335418.16	335418.16	1341672.65
primary load x [N]	0.00	0.00	0.00	0.00	
Primary load y [N]	-175.00	-175.00	-175.00	-175.00	-700.00
x' [mm]	-16.00	0.00	16.00	0.00	
y' [mm]	0.00	16.00	0.00	-16.00	
r [mm]	16.00	16.00	16.00	16.00	
rGA [Nm]	5366690.61	5366690.61	5366690.61	5366690.61	
r2GA [Nmm2]	85867049.73	85867049.73	85867049.73	85867049.73	343468198.93
secondary load [N]	-1246.88	-1246.88	-1246.88	-1246.88	
secondary load on x axis [N]	0.00	1246.88	0.00	-1246.88	
secondary load on y axis [N]	1246.88	0.00	-1246.88	0.00	
sum of forces in X axis [N]	0.00	1246.88	0.00	-1246.88	0.0
sum of forces in Y axis [N]	1071.88	-175.00	-1421.88	-175.00	-700.0
total force [N]	1071.88	1259.10	1421.88	1259.10	

Table 6. Theoretical loads on eccentric joint.

2) Rivet reserve factor:

According to Avex, rivet max allowable load is 1000 newtons, from this data reserve factors are calculated:

$RF_{c1} = \frac{F_r}{F_{rc1}} = 0.93 \quad RF_{c2} = \frac{F_r}{F_{rc2}} = 0.79 \quad RF_{c3} = \frac{F_r}{F_{rc3}} = 70 \quad RF_{c4} = \frac{F_{r1}}{F_{rc4}} = 0.79$ where F_r-max allowable rivet load [N] F_{rcn}- given number of traditionally calculated rivet load.

	RF 1	RF2	RF 3	RF 4
Traditional approach	0.93	0.79	0.70	0.79

Table 7. Reserve factors of each rivet

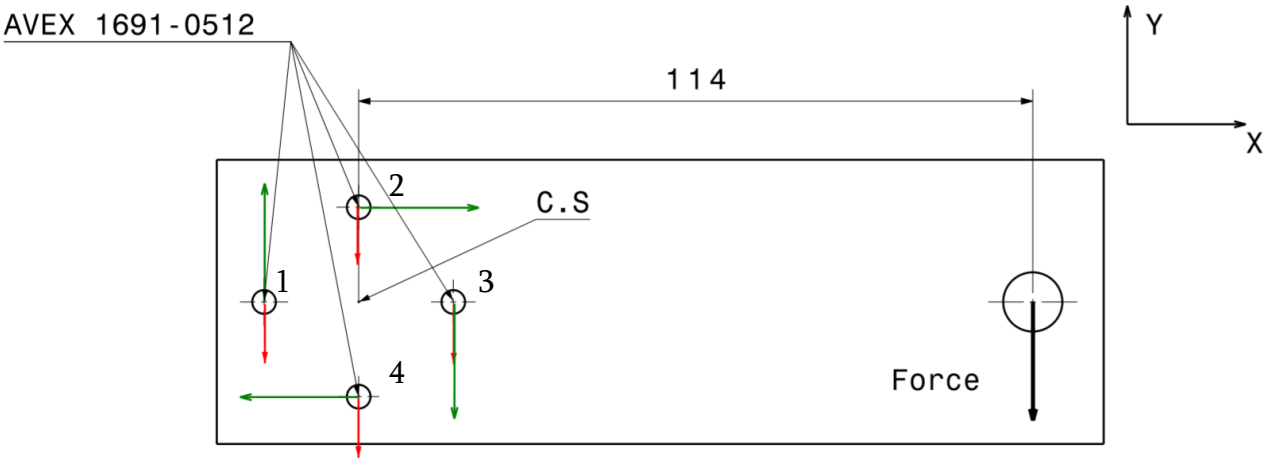

Figure 41. Force vectors (red arrows represent primary load, green-secondary).

5.3.2. Finite element models

In the first two joint FE models for sheet description, 2D shell QUAD4 elements are used with 2mm of element of thickness, on sheet geometry rivet holes were also applied, for rivet – at first analysis the CBUSH elements, properties are shown in Table 8 element orientation is <1 0 0>, at the second analysis the CBEAM elements, property for that element is: rod cross section with radius of 2mm element orientation same as CBUSH. At the first attempt rivet and sheet are connected with the RBE3 element (Figure 42), on second try with the RBE2. The model is fixed at one and in every translational and rotational direction, while the other end, where the force is applied in y direction, is free in every direction as real test is made. whole model is shown in Figure 67. The force itself is static, analysis is performed with 5 load cases: 400, 500, 600, 700 and 800 newtons. The analysis is done with 106 nonlinear solution. Results are shown in Figure 43, Figure 44, Table 9 and Table 10.

D [mm]	4
E [MPa]	71000
G [MPa]	26691.73
A [mm2]	12.57
As=3A/4 [mm2]	9.42
L [mm]	2.00
I [mm4]	12.57
J [mm4]	25.13
KT1 [Nmm-1]	446106.16
KT2 [Nmm-1]	125781.81
KT3 [Nmm-1]	125781.81
KR1 [Nmm]	335418.16
KR2 [Nmm]	613815.24
KR3 [Nmm]	613815.24

Table 8. Spring constants

Rivet number	1	2	3	4	∑
sum of forces in X axis [N]	0.00	1246.88	0.00	-1246.88	0.00
sum of forces in Y axis [N]	1071.88	-175.00	-1421.88	-175.00	-700.00
total force [N]	1071.88	1259.10	1421.88	1259.10	
FEM CBUSH force on X axis [N]	2.43	-1401.80	-1.90	1401.30	0.03
FEM CBUSH force on Y axis [N]	855.31	-153.03	-1253.90	-148.41	-700.03
FEM CBUSH magnitude force [N]	855.31	1410.20	1253.90	1409.20	
CBUSH difference on X axis [%]	0.00	12.43	0.00	12.38	
CBUSH difference on Y axis [%]	20.20	12.55	11.81	15.19	
BUSH difference of total force Cbush [	20.20	12.00	11.81	11.92	
FEM CBEAM force on X axis [N]	-0.02	-1261.70	-0.02	1261.70	-0.03
FEM CBEAM force on Y axis [N]	1030.70	-171.58	-1387.60	-171.59	-700.07
FEM Cbeam force [N]	763.25	1480.90	1188.00	1479.30	
Difference of total force Cbeam [%]	28.79	17.62	16.45	17.49	

Table 9. Comparison of Theoretical and FEM results (with RBE3 elements)

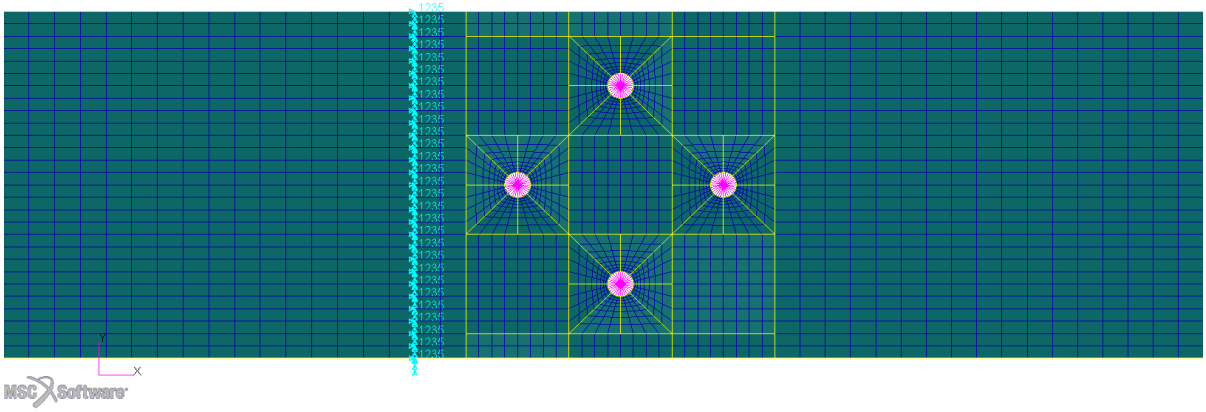

Figure 42. Eccentric configuration with rivet holes in the model

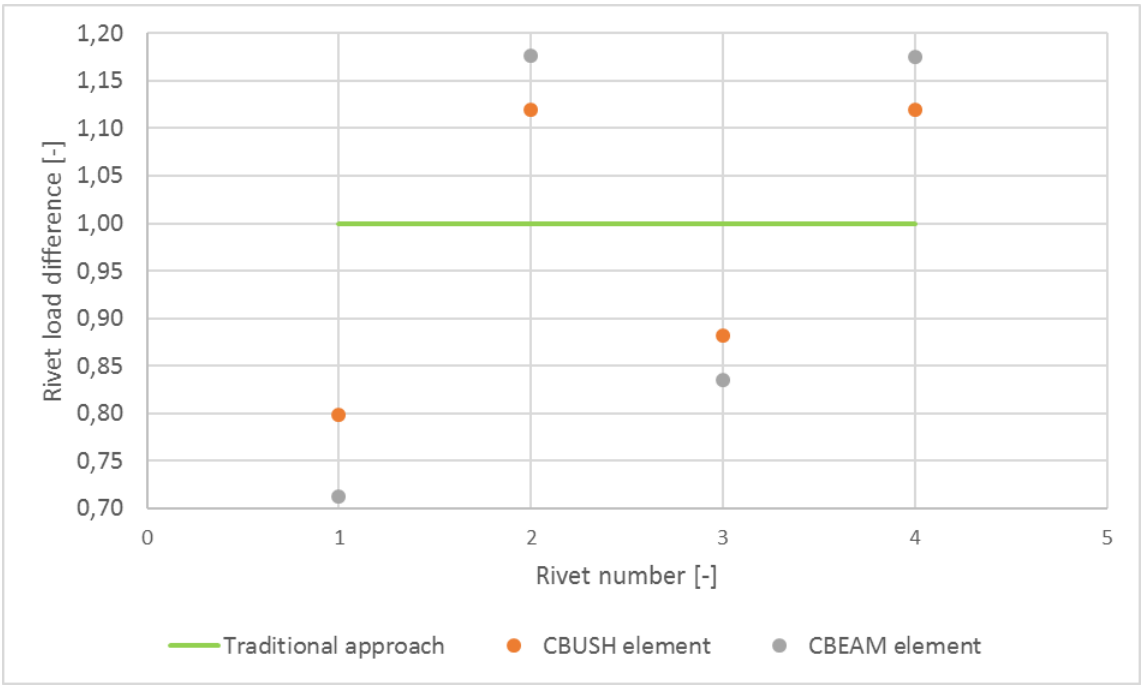

Figure 43. Eccentric configuration FEM results with RBE3 element and with rivet holes.

Rivet number	1	2	3	4	∑
sum of forces in X axis [N]	0	1246.875	0	-1246.875	0
sum of forces in Y axis [N]	1071.875	-175	-1421.875	-175	-700
total force [N]	1071.875	1259.0958	1421.875	1259.0958	
FEM Cbush force on X axis [N]	2.22	-1387.10	-1.93	1386.80	-0.0061
FEM Cbush force on Y axis [N]	-871.75	154.75	1266.60	150.36	699.96
FEM Cbush magnitude force [N]	871.75	1395.80	1266.60	1395.00	
Cbush difference on X axis [%]	0	11.246115	0	11.222055	
Cbush difference on Y axis [%]	181.33	188.43	189.08	185.92	
Cbush difference of total force Cbush [%]	18.670554	10.85733	10.92044	10.793792	
FEM CBEAM fore on X axis [N]	3.8031	-1454.9	-3.5229	1454	-0.6198
FEM CBEAM fore on Y axis [N]	785.1	-141.12	-1204.5	-139.46	-699.98
FEM Cbeam force [N]	785.11	1461.9	1204.5	1460.7	
Difference of total force Cbeam [%]	26.753586	16.107129	15.287912	16.011823	

Table 10. Comparison of Theoretical and FEM results (with RBE2 elements)

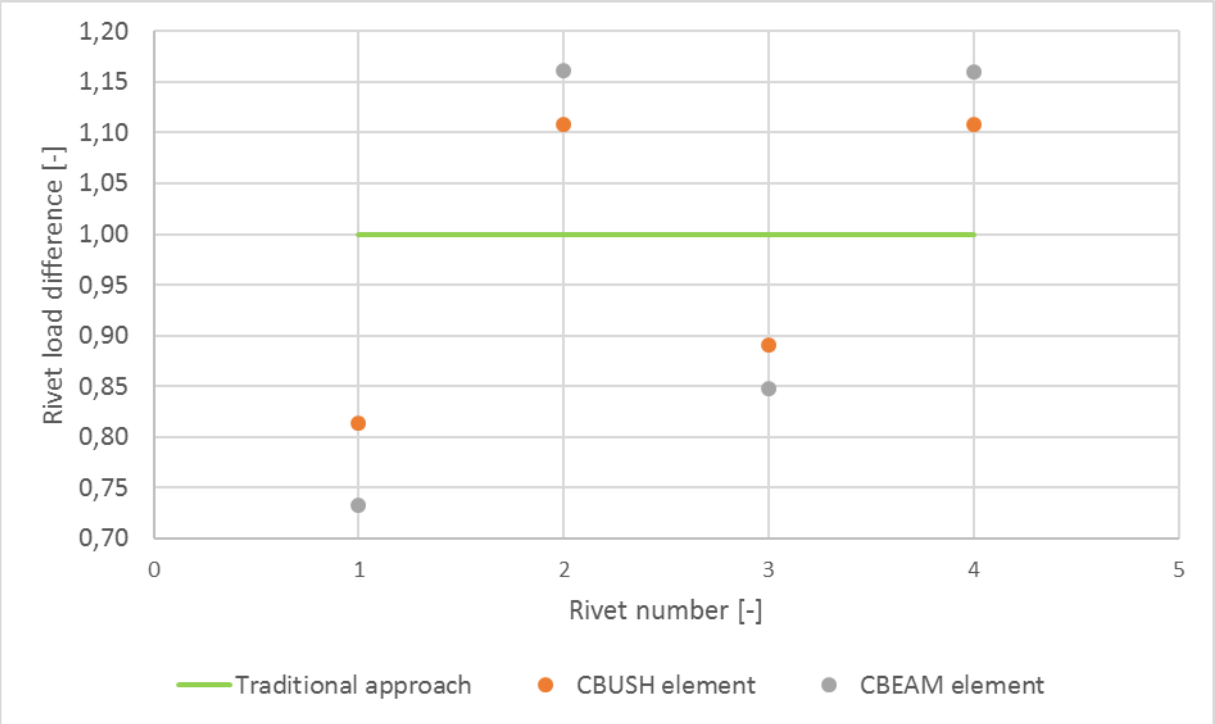

Figure 44. Eccentric configuration FEM results with RBE2 element and with rivet holes.

In the next two models' same the elements and properties are used, in the geometry rivet holes are not considered (Figure 45). Results are shown in Figure 46, Figure 47, Table 11 and Table 12.

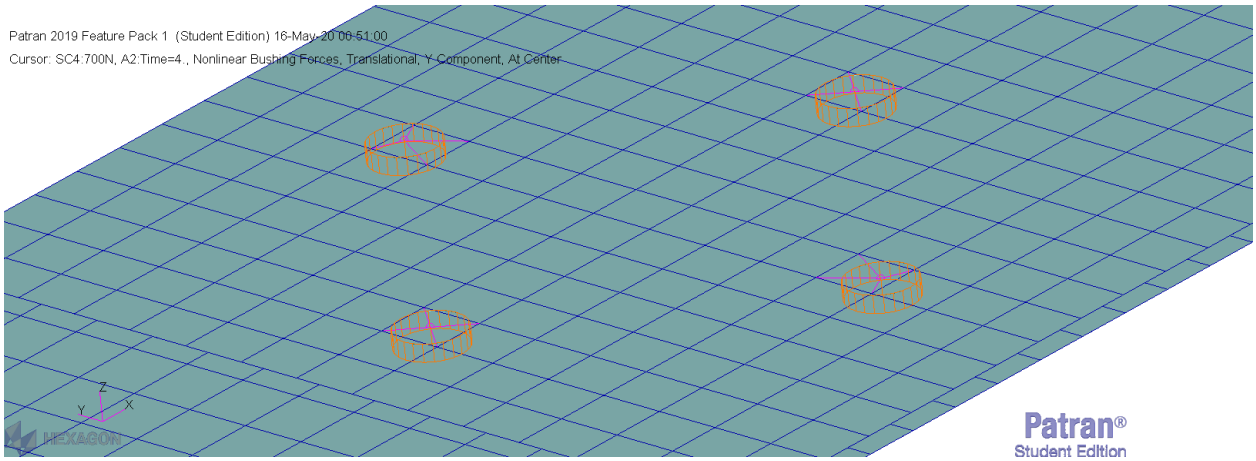

Figure 45. FE model with RBE elements and without rivet holes in the model.

Rivet number	1	2	3	4	∑
sum of forces in X axis [N]	0.00	1246.88	0.00	-1246.88	0.0
sum of forces in Y axis [N]	1071.88	-175.00	-1421.88	-175.00	-700.0
total force [N]	1071.88	1259.10	1421.88	1259.10	
FEM Cbush force on X axis [N]	2.55	-1397.70	-2.35	1397.50	0.0
FEM Cbush force on Y axis [N]	-866.43	153.44	1263.90	149.10	700.0
FEM Cbush magnitude force [N]	866.43	1406.10	1263.90	1405.50	
Cbush difference on X axis [%]	0.00	12.10	0.00	12.08	
Cbush difference on Y axis [%]	180.83	187.68	188.89	185.20	
Cbush difference of total force Cbush [%]	19.17	11.68	11.11	11.63	
FEM CBEAM force on X axis [N]	4.26	-1474.70	-4.02	1473.80	-0.7
FEM CBEAM force on Y axis [N]	774.37	-138.39	-1199.40	-136.53	-700.0
FEM Cbeam force [N]	774.38	1481.20	1199.50	1480.10	
Difference of total force Cbeam [%]	27.75	17.64	15.64	17.55	

Table 11. Comparison of Theoretical and FEM results (with RBE3 elements, without rivet holes)

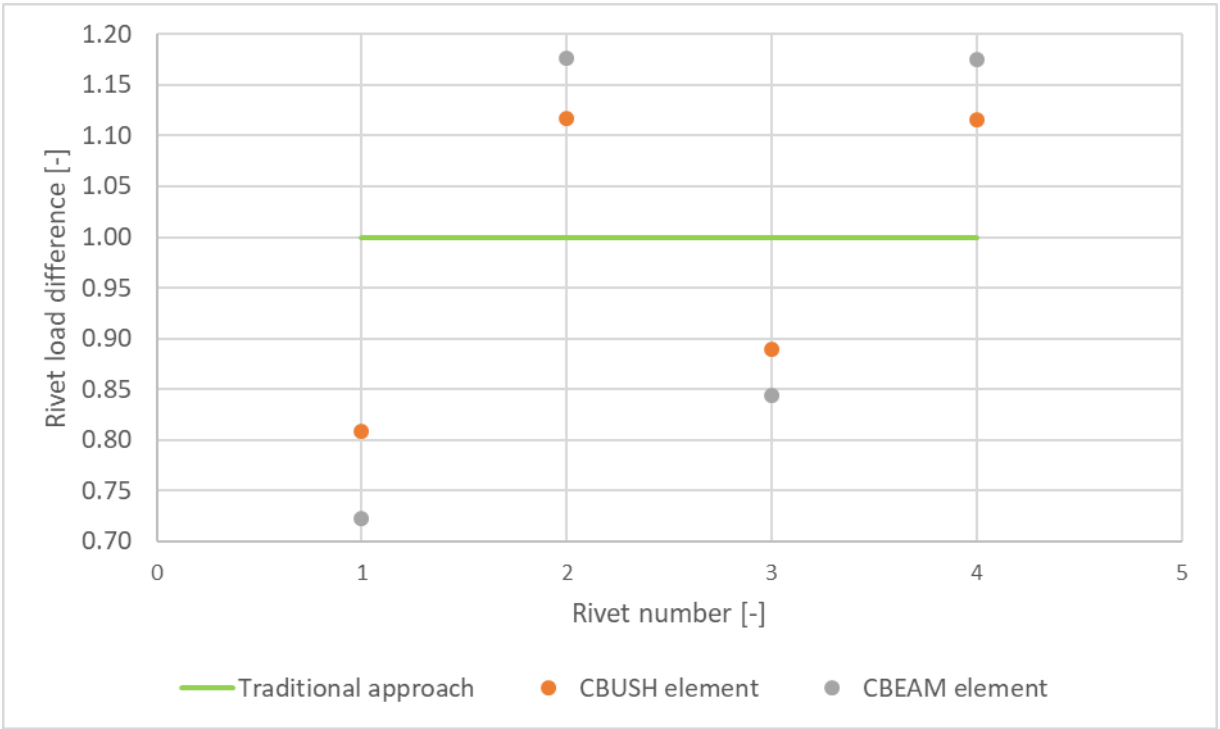

Figure 46. Eccentric configuration FEM results with RBE3 element and without rivet holes.

Rivet number	1	2	3	4	∑
sum of forces in X axis [N]	0.00	1246.88	0.00	-1246.88	0.00
sum of forces in Y axis [N]	1071.88	-175.00	-1421.88	-175.00	-700.00
total force [N]	1071.88	1259.10	1421.88	1259.10	
FEM Cbush force on X axis [N]	2.37	-1391.60	2.28	1391.60	4.65
FEM Cbush force on Y axis [N]	-873.31	153.98	1269.60	149.77	700.04
FEM Cbush magnitude force [N]	873.31	1400.20	1269.60	1399.60	
Cbush difference on X axis [%]	0.00	11.61	0.00	11.61	
Cbush difference on Y axis [%]	18.53	12.01	10.71	14.42	
Cbush difference of total force Cbush [%]	18.53	11.21	10.71	11.16	
FEM CBEAM force on X axis [N]	4.03	-1467.10	-4.04	1466.50	-0.61
FEM CBEAM force on Y axis [N]	-783.15	139.25	1206.50	137.41	700.01
FEM Cbeam total force [N]	783.20	1473.80	1206.50	1472.90	
Difference of total force Cbeam [%]	26.93	17.05	15.15	16.98	

Table 12. Comparison of Theoretical and FEM results (with RBE2 elements, without rivet holes)

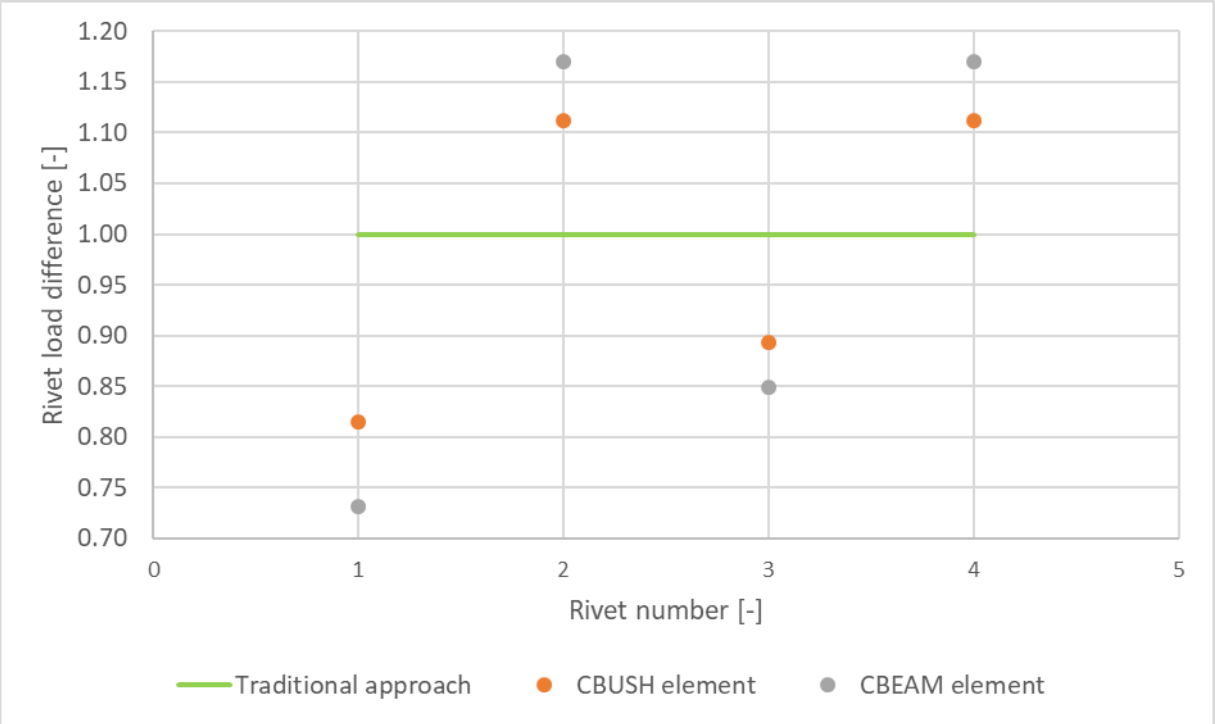

Figure 47. Eccentric configuration FEM results with RBE2 element and without rivet holes.

In the last model rivet to sheet connection are node to node as shown in Figure 48, without any MPC element. Results are shown in Figure 49 and Table 13.

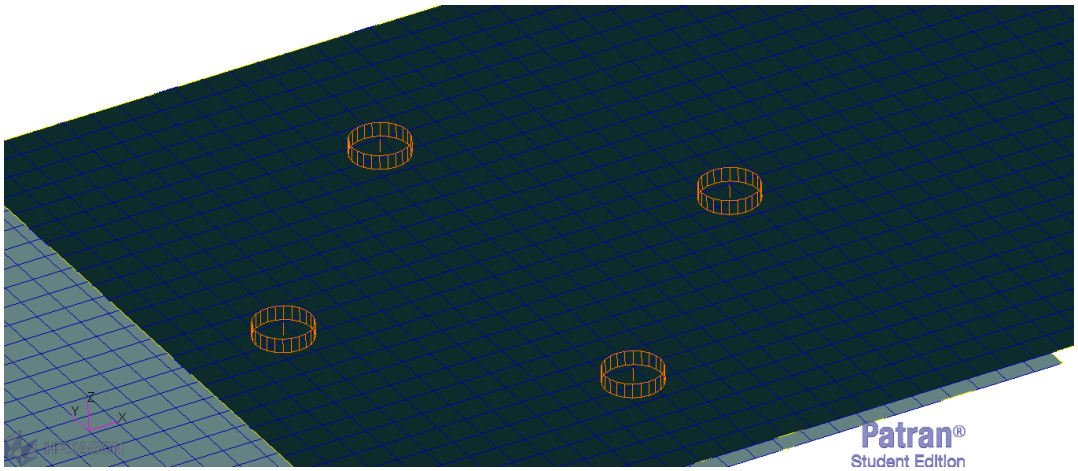

Figure 48. Node to node connection

Rivet number	1	2	3	4	∑
sum of forces in X axis [N]	0.00	1246.88	0.00	-1246.88	0.00
sum of forces in Y axis [N]	1071.88	-175.00	-1421.88	-175.00	-700.00
total force [N]	1071.88	1259.10	1421.88	1259.10	
FEM CBUSH force on X axis [N]	1.11	-1378.80	-1.58	1379.30	0.02
FEM CBUSH force on Y axis [N]	919.75	-156.86	-1309.50	-153.41	-700.02
FEM CBUSH magnitude force [N]	919.75	1387.80	1309.50	1387.90	
CBUSH difference on X axis [%]	0.00	10.58	0.00	10.62	
CBUSH difference on Y axis [%]	14.19	10.37	7.90	12.34	
CBUSH difference of total force Cbush [%]	14.19	10.22	7.90	10.23	
FEM CBEAM force on X axis [N]	2.99	-1421.50	-4.37	1422.00	-0.88
FEM CBEAM force on Y axis [N]	-869.56	147.22	1274.20	148.08	699.94
FEM CBEAM force [N]	869.56	1429.30	1274.30	1429.70	
Difference of total force CBEAM [%]	18.87	13.52	10.38	13.55	

Table 13. Comparison of Theoretical and FEM results (node to node connection)

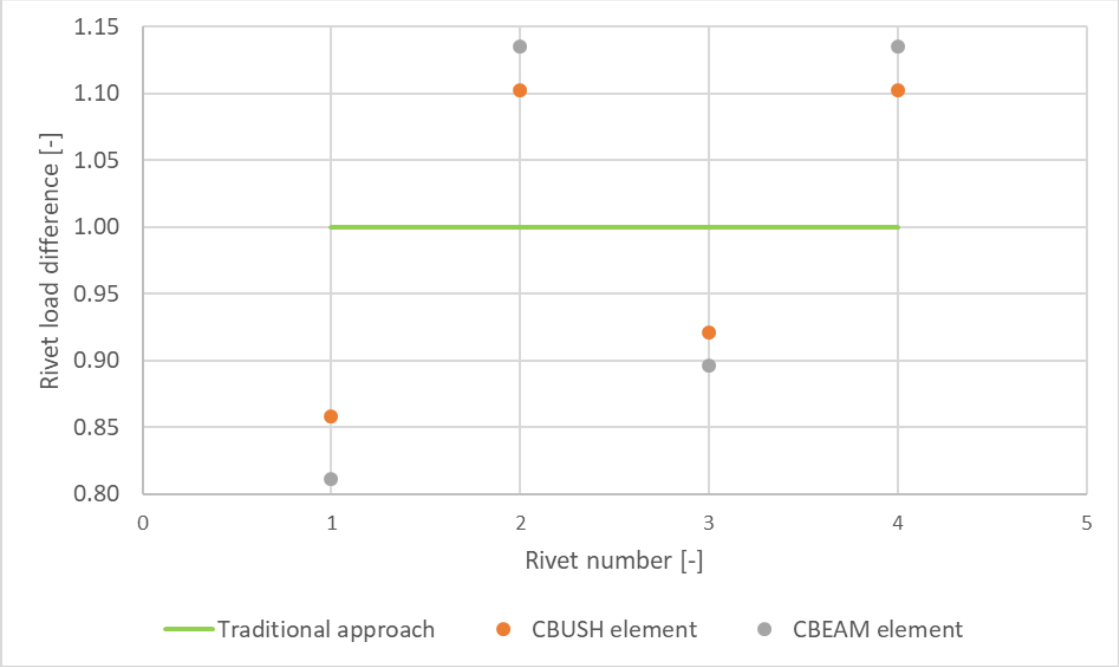

Figure 49. Eccentric configuration FEM results of node to node connection.

In these results difference is much greater than previous configurations, apart from mentioned errors, here main error is that joint is not perfectly rigid and sheet deformation has its own impact, to compare Figure 68 represents model where sheet thickness is 2 mm which is used in real static tests, while Figure 69 represents model where sheet thickness is 50 mm (much closer to be "perfectly rigid"), this modification affected on rivet loads significantly, on 700 newton load CBUSH elements had next forces : 1-1045.7 [N] 2-1257.5 [N], 3-1398.7 [N], 4-1257.4 [N], where 1,2,3,4 are rivets numbering. As it can be seen its much closer with traditional calculation values.

To sum up the best model among mentioned ones still is model where node to node connection is used, because its accuracy and simplicity. It is hard to choose between CBEAM and CBUSH elements, as difference between them is quite small (less than 5%). But still because CBUSH is closer to traditional approach, CBUSH can be considered better element than CBEAM.

6. Static testing

Both methods above traditional approach and FE analysis need to be proved with real static tests, which were performed in Brno University of Technology. Unfortunately, the only information rivet producer has is minimum load (1000 newton), which can withstand one rivet. Parallel and serial configurations were tested in static test machine. Relation between force and elongation from that data is shown in Figure 52 and Figure 55. For this type of test its easier to distinguish were elastic region ends and plastic deformation starts as data is stored in computer every 0.01 second. For eccentric configuration, because of inconvenient structure, it was tested with method of "loading by weight" (Figure 57), that's why extra holes where made on structure to obtain good fixation and to apply load. From this testing only force, failure was detected, failure forces for eccentric configuration are shown in Table 14. During eccentric joint test, all specimens failed completely when 1 most loaded rivet failed and then very fast, almost immediately, all other rivets failed. Structure geometries are shown in Figure 50, Figure 53 and Figure 56. Samples after failure are shown in Figure 51,Figure 54 and Figure 59. All structures sheets were quite strong to obtain only rivet shear failure. Standard deviations were calculated and visualized in Table 15 and Figure 58. As mentioned above rivet producer only gave minimum load, under which rivet will have shear failure. So that means company gave minimum value of negative standard deviation interval on bell shaped curve.

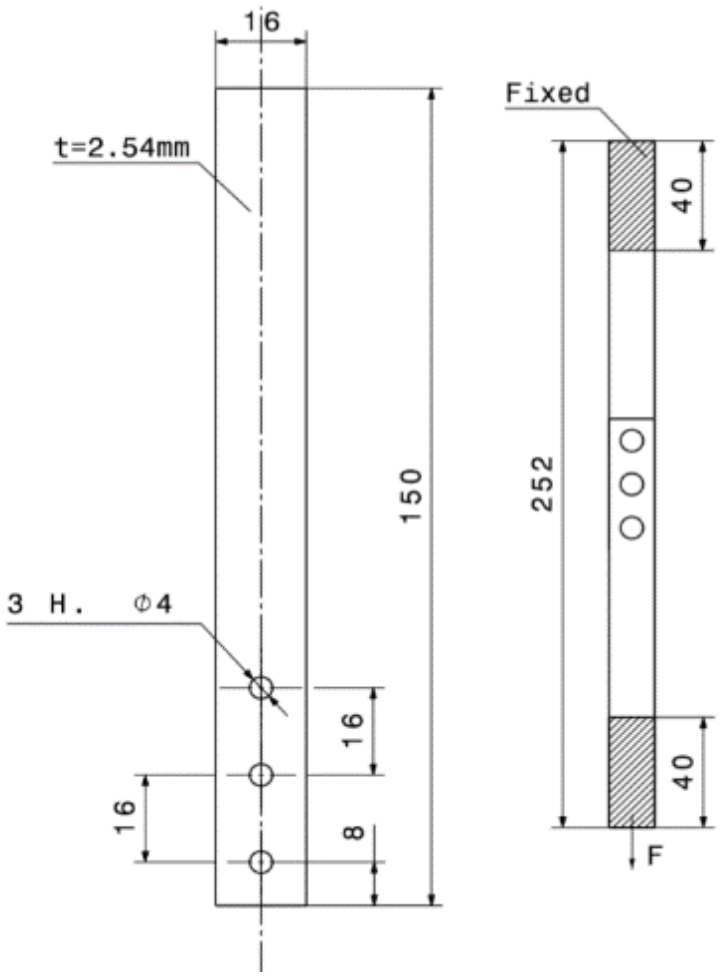

Figure 50. Three rivets in serial configuration drawings

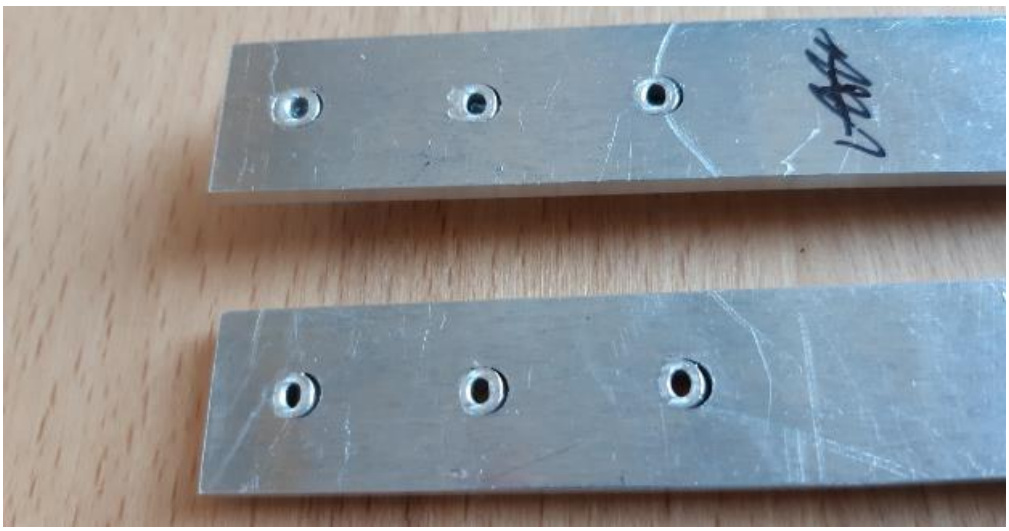

Figure 51. Three rivets in serial configuration after static test

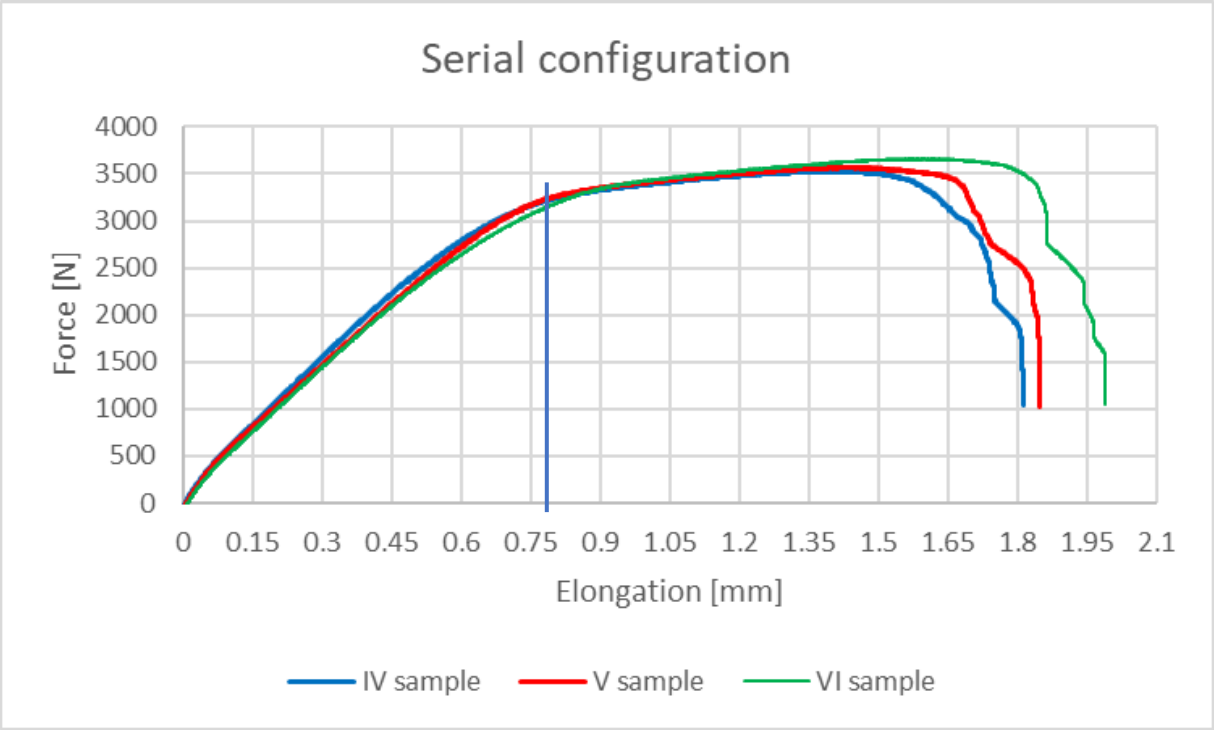

Figure 52. Joint in serial configuration. (vertical blue line - end of the elastic region).

Attempts	Eccentric conf.
1	700 Newtons
2	730 Newtons
3	800 Newtons

Table 14. Failure force for eccentric configuration joint samples

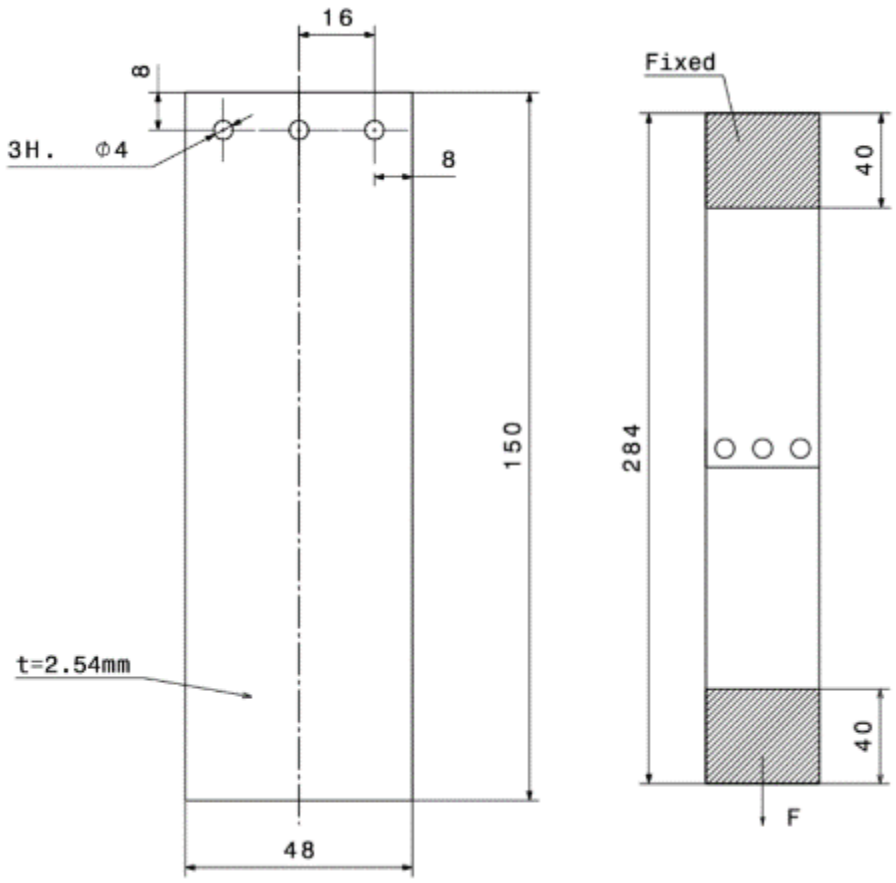

Figure 53. Three rivets in parallel configuration drawing.

Figure 54. Three rivets in parallel configuration after static test.

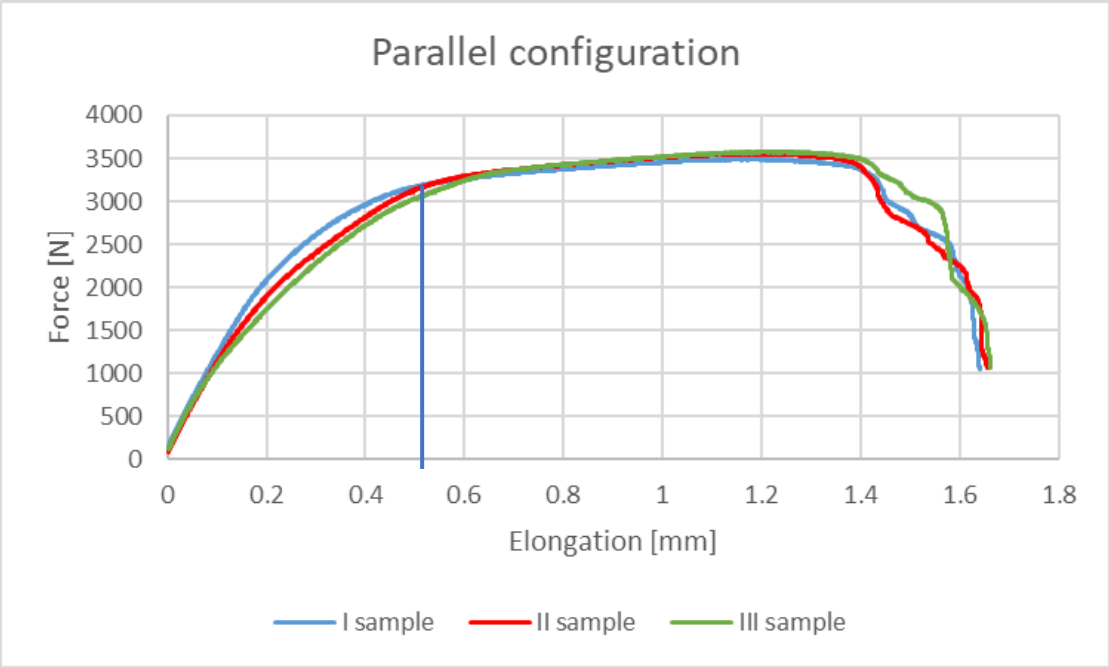

Figure 55. Joint in parallel configuration. (vertical blue line - end of the elastic region)

Attempts	Eccentric conf.	Serial conf.	Parallel conf.
1	700	3535.5	3494.5
2	730	3574.5	3563.5
3	800	3668	3580
Mean	743.33	3592.67	3546.00
Standard dev.	51.32	68.09	45.36

Table 15 Failure forces for all configuration joints and their standard deviations

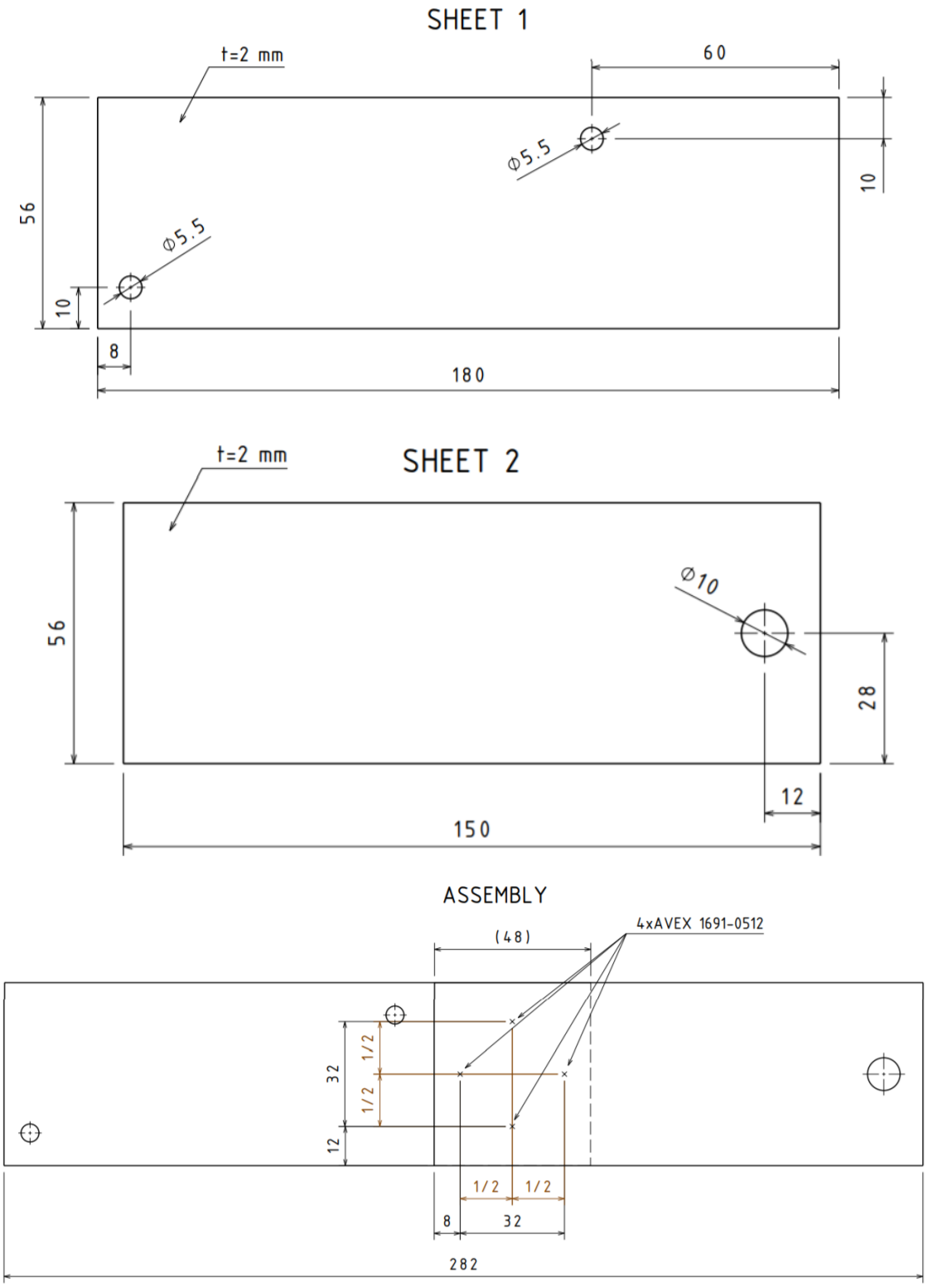

Figure 56. Eccentric configuration drawing.

Figure 57. Static test of the eccentric configuration joint

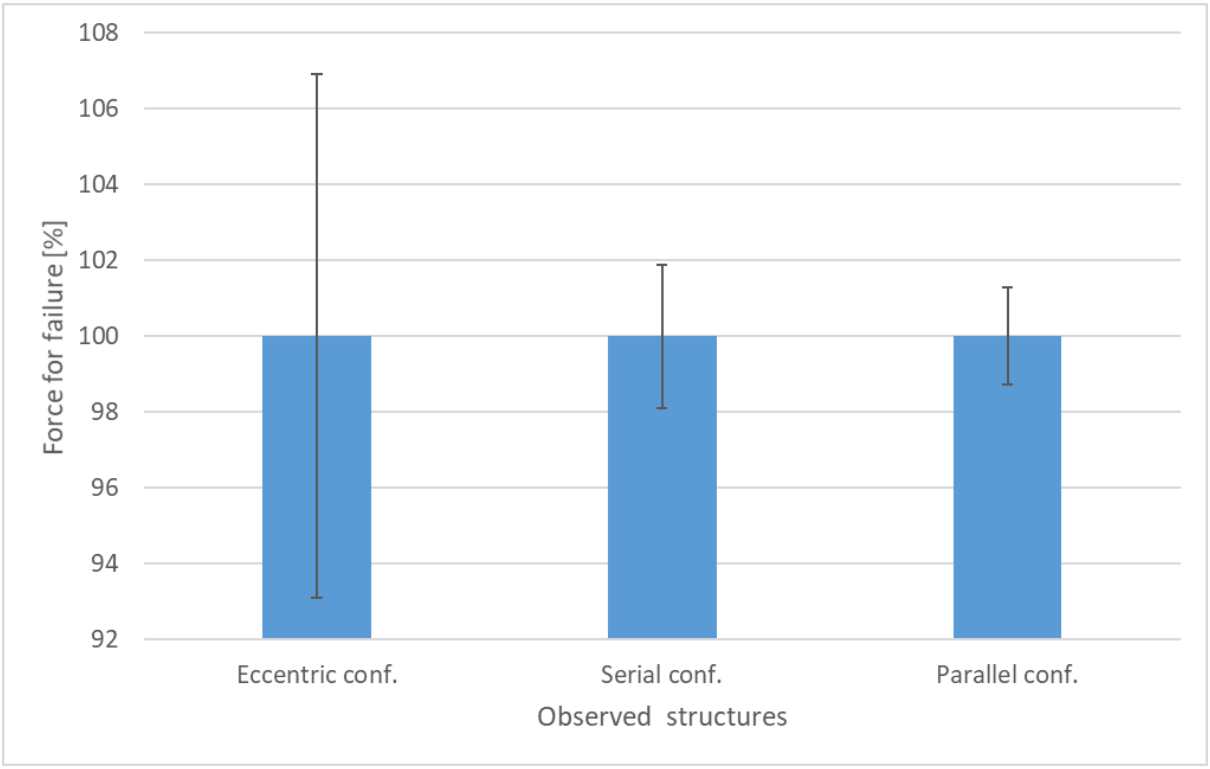

Figure 58. Standard deviation results of all configuration static tests.

Figure 59. Eccentric configuration lap joint after static test.

From rivet supplier only minimum force is known under which rivet might fail (a rivet might fail under higher force than force given by the supplier). According with data from static tests and previous analysis all structure failed after at least one rivet reached 1000 newton load. From standard deviation graph (figure 58), reason why eccentric configuration has bigger gap on standard deviation than the parallel and serial configuration is arm of the bending moment, because small increase of the input load will lead to a bit bigger rivet load increase, than input load, plus joint is not perfectly rigid and the deformation of the sheet changes rivets load. But even with this influence rivets didn't fail before reaching minimum load. It can be said that from all mentioned models above, node to node connection is better model than the others, due to it is much simpler to model than the others and has closer results compare with the traditional analysis.

Conclusion

This thesis has focused on finding optimal models of three different configurations of the rivet joint in MSC Nastran/Patran software. These models have to be the verification step of the previous traditional analysis in order to give the engineer a better understanding of the joint behavior under some load, which leads to the reduction of next "static test" step time and budget.

The traditional analysis is quite conservative and has some idealized conditions, for example in rivet joint analysis joint is assumed to be perfectly rigid. The FEA proves that with the "perfect rigidity" values of FEM results and the traditional calculation is quite similar. However, in reality, the structure deforms, which produces an extra unknown force that is why the joint with 2 mm thickness of the sheet had much bigger difference results than 50 mm. In case when those extra unknown forces are not considered, there is a possibility that one specimen will brake earlier than expected, which leads in one solution to increase rivets diameter or other cases sheet thickness, which itself leads to the weight and budget penalty.

The engineer must know the criteria in which he/she needs to design the structure. According to the models which were used in this paper, the main concern was the rivet shear failure, therefore, stresses around rivet holes were not crucial (that is why the extra RBE elements can be neglected), in comparison to the traditional calculations - sheets of which were quite strong compared with

the rivets. However, according to the received data, it was proven that even though there were quite strong sheets, their deformation made induced extra forces, which were not included in the traditional analysis. This effect is quite noticeable when in eccentric configuration FE model sheet stiffness were increased 25 times (structure got closer to be called “perfect rigid”).

As the FE analysis is still called a new tool, I believe in the near future, apart from the element descriptions, there will be documents, where the exact elements will be highlighted in order to describe the types of structures, with the practical examples to make the more precise models for the better understanding of the product behaviour.

The findings in this paper links theoretical materials (traditional approaches and understanding of finite element method) each other in order to approach to a more realistic results and to reduce the number of the specimens tested in the laboratory to the minimum. It should be considered that in this case only the static test was performed. During the later stage a fatigue and dynamic analysis in Finite Element Method could also be performed.

Among the above-mentioned FE models, it becomes clear that the node to node connection is better than the others. The reason for that is the chosen criteria “rivet shear failure”. The chosen models should not require the rivet holes, but only the exact rivet and load locations on sheet and the properties of the structural parts are important, for the purposes to make sure that traditional analysis steps are considered and its error of having the perfect rigidity is neglected. In the serial and parallel configuration, the real static tests results are quite similar, because there are slight differences in the load distribution according to FE and traditional analysis. However, in case of the eccentric configuration, the difference is much greater as bending moment produces a deformation that leads an extra induced force.

Considering all the above-mentioned, we may come to the conclusion that under the performance of the tool discussed in the paper, shall enable us to better understand structure behavior under specific load. The finding shall reduce the engineer’s faults and offer the chance to have the best possible result with much less cost in terms of both time and materials used, making the latter a better way in comparison to already established traditional approaches.

References

[1] CHUN-YUNG NIU, Michael, Airframe Stress Analysis and Sizing, second edition, Hong Kong: Conmilit Press LTD. 1999, ISBN 962-7128-08-2;

[2] CHUN-YUNG NIU, Michael, Airframe Structural Design, Hong Kong: Conmilit Press LTD. 1988, ISBN 762-7128-04-X;

[3] DIMAROGONAS, Andrew D., Machine Design a CAD Approach, New York: John Wiley & Sons, INC. 2001, ISBN 0-471-31528-1;

[4] MIL-HDBK-5H, Military Handbook: Metallic Materials and Elements for Aerospace Vehicle Structures. Available from: http://everyspec.com/MIL-HDBK/MIL-HDBK-0001-0099/MIL_HDBK_5H_1804/;

[5] CS-23, Certification Specifications for Normal, Utility, Aerobatic, and Commuter Category Aeroplanes, Amendment 3, 2012. Available from: https://www.easa.europa.eu/certification-specifications/cs-23-normal-utility-aerobatic-and-commuter-aeroplanes;

[6] BRUHN, Elmer Franklin. Analysis and design of flight vehicle structures. Cincinnati: Tri-State Offset Co, [1965];

[7] Linear Static analysis User's Guide, MSC Nastran, 2019, NA:V2019.1:Z:Z:Z:DC-LIN-PDF;

[8] Quick Reference Guide, MSC Nastran, 2018, NA:V2018:Z:Z:DC-QRG-PDF.

LIST OF FIGURES

LIST OF TABLES

APPENDIX

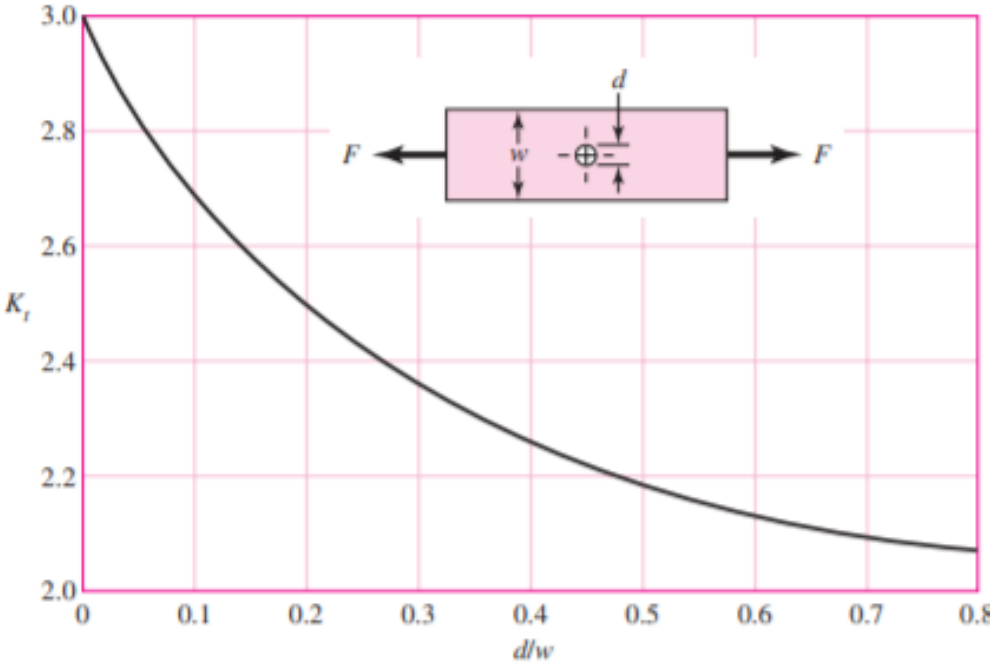

Figure 60. Theoretical concentration factor

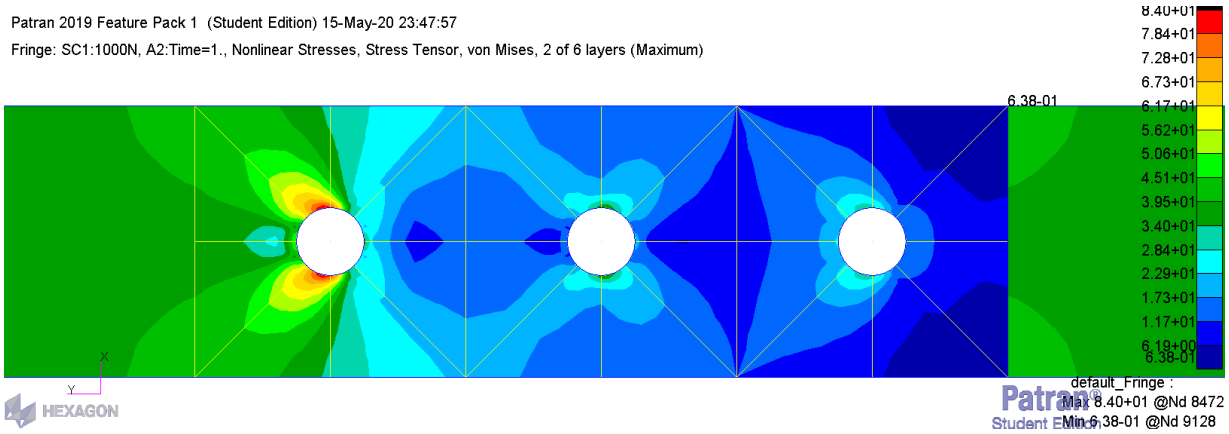

Figure 61. Stress distribution with RBE3 elements

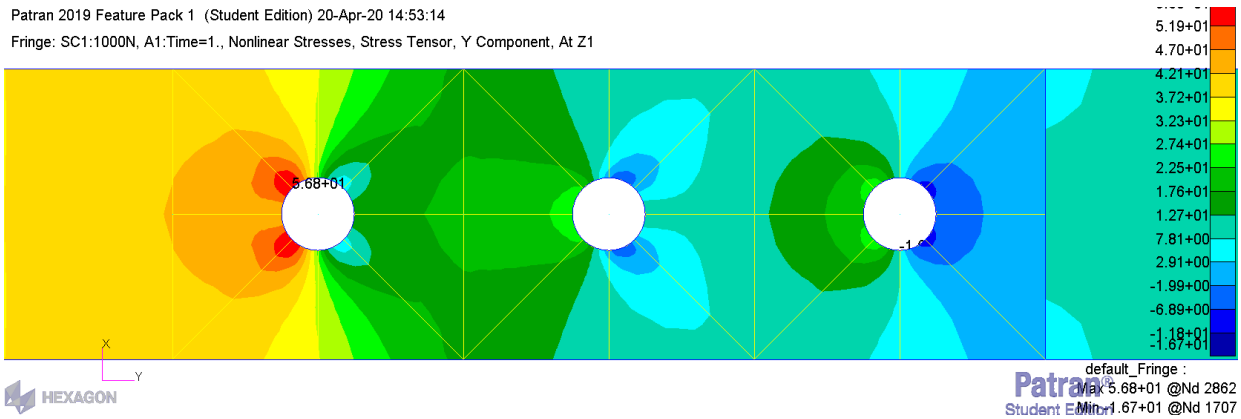

Figure 62. Three rivets in parallel. Stress distribution with RBE2 element

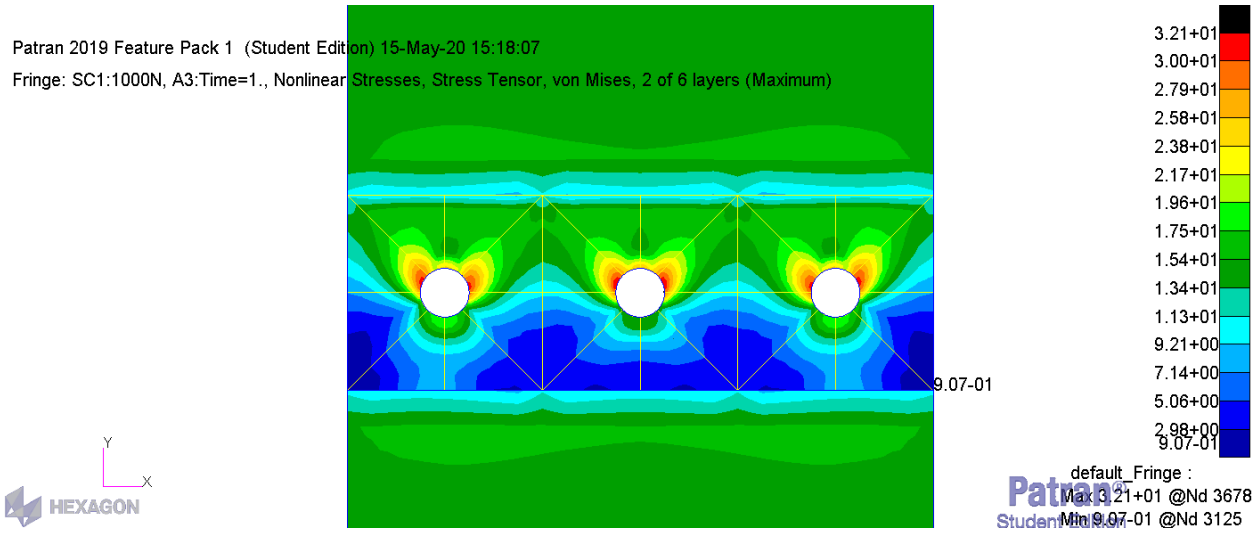

Figure 63. Three rivets in parallel. Stress distribution with RBE3 element

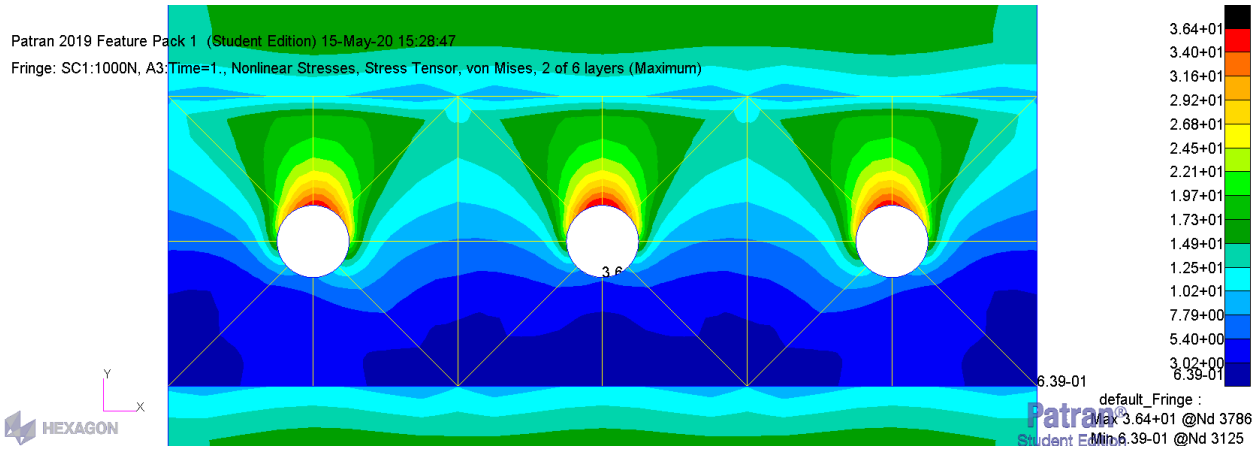

Figure 64. Three rivets in parallel. Stress distribution with RBE2 element

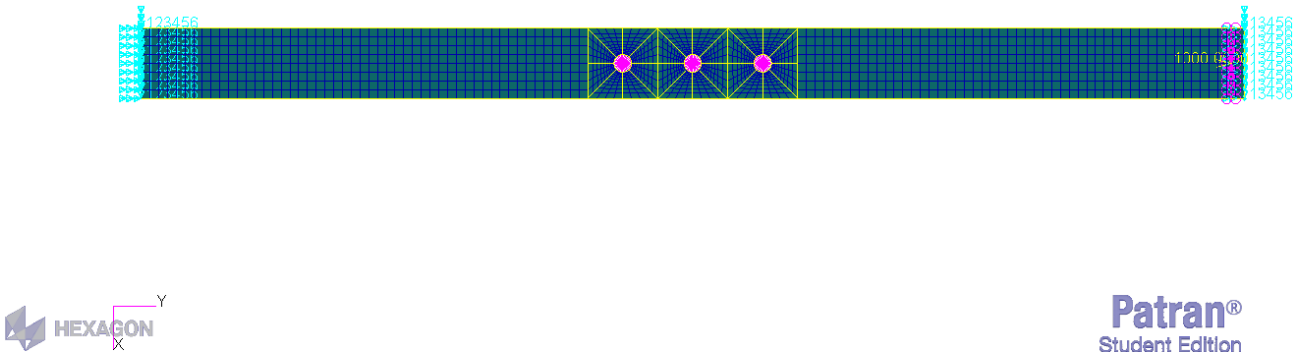

Figure 65. Three rivets in serial configuration. FE model.

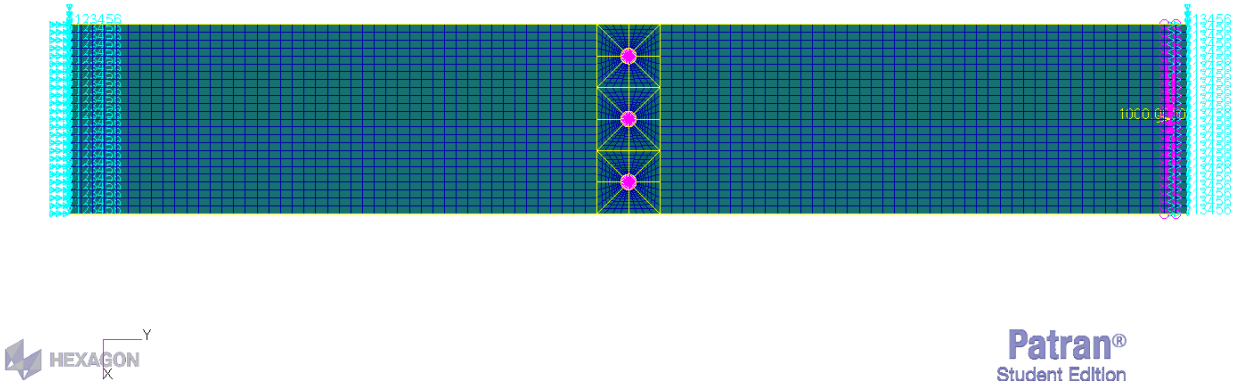

Figure 66. Three rivets in parallel configuration. FE model.

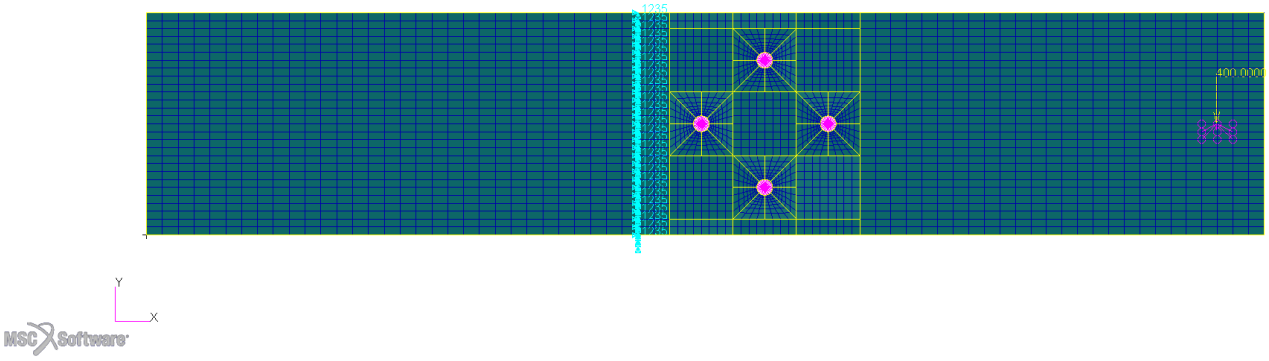

Figure 67. Three rivets in eccentric configuration. FE model

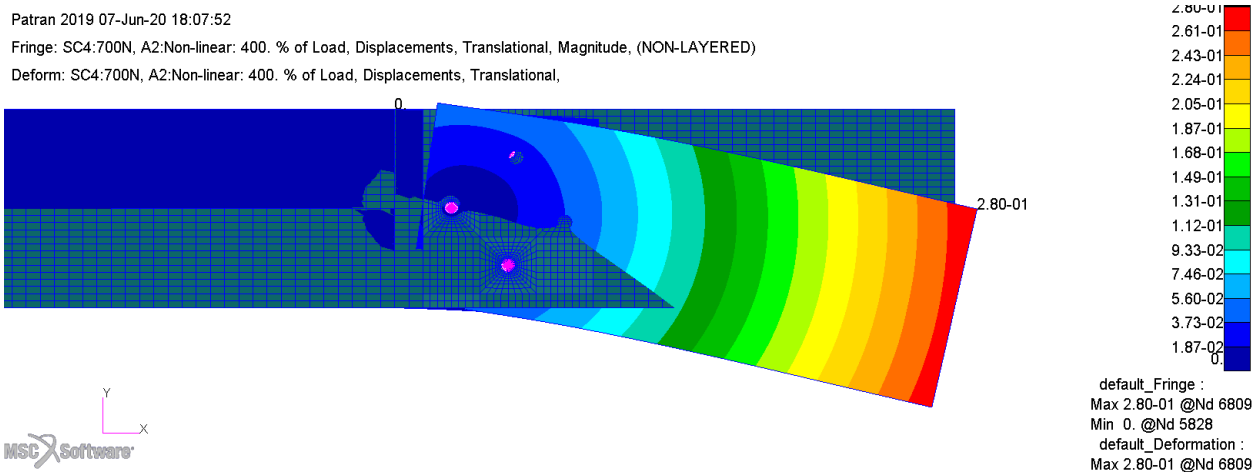

Figure 68. Displacement with 2mm sheet thickness

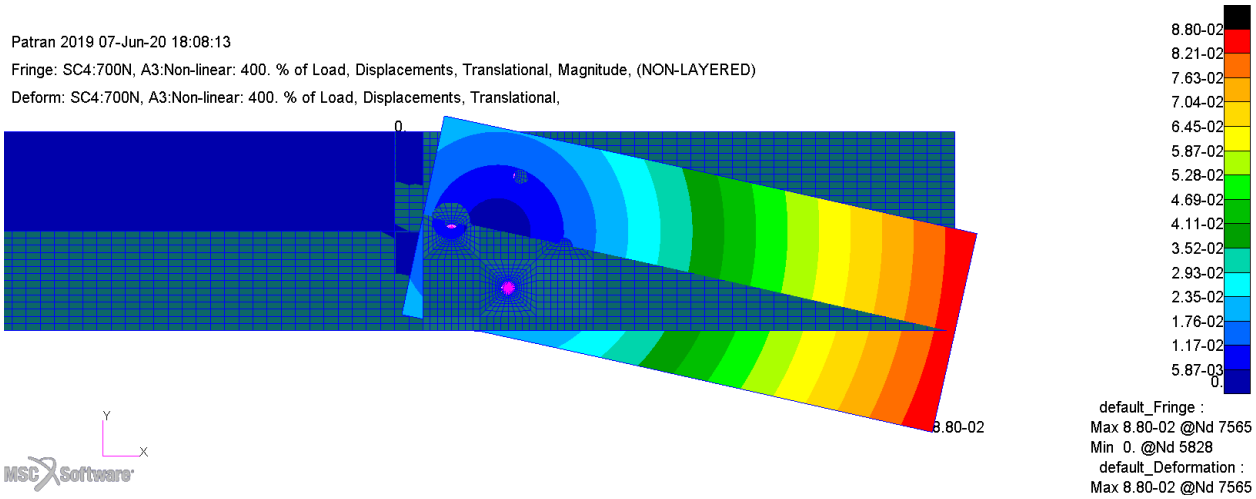

Figure 69. Displacement with 50mm sheet thickness